A Platinum Open Access Journal for Organic Chemistry

Review

Free to Authors and Readers | DOAJ Seal | *Arkivoc* **2025** (2) 202612586

Sustainable chemical transformations: unconventional bio-based solvents in photo- and electrochemistry

Jhonathan R. N. dos Santos,[a] Carlos Eduardo T. Rosa,[a] Éverton A. Tordato[a,b] and Arlene G. Corrêa[a]*

[a]Centre of Excellence for Research in Sustainable Chemistry, Department of Chemistry, Federal University of São Carlos, São Carlos, 13565-905, SP, Brazil; [b] University of São Paulo, São Paulo, 05403-900, SP, Brazil
Email: agcorrea@ufscar.br

This review is dedicated to Dr. Rajender Varma, whose pioneering contributions to green chemistry have played an important role in inspiring and supporting the establishment of the Centre of Excellence for Research in Sustainable Chemistry at Federal University of São Carlos in Brazil

Received 03-16-2026 **Accepted** 06-08-2026 **Published on line** 06-15-2026

Abstract

The global goal of sustainable development can be facilitated, within the context of chemical processes, through the adoption of bio-based solvents, since they are derived from renewable sources, biodegradable and safer than petrochemical based solvents. In this review, we covered studies published between 2020-2025 in which less explored or emerging bio-based solvents were used, with a particular focus on their applications in photo- or electrochemical transformations, as well as discussions on mechanistic aspects.

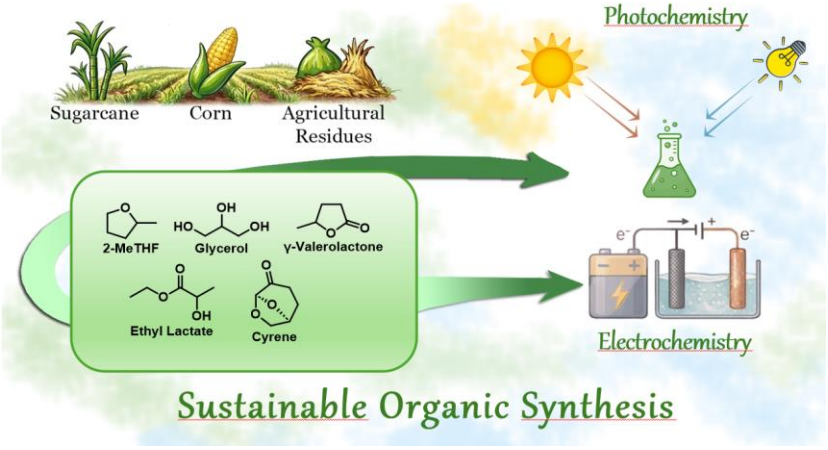

Keywords: bio-based solvents; photochemistry; electrochemistry; green chemistry

Cite as *Arkivoc* **2025** (2) 202612586
DOI: https://doi.org/10.24820/ark.5550190.p012.586

Table of Contents

1. Introduction

Over the last decades, advances allowed the efficient construction of C–C and C–heteroatom bonds, important in synthetic drugs and bioactive compounds, enabling access to increasingly complex compounds.[1,2] However, many of these transformations present drawbacks, from low selectivity and thermodynamic stability to reactive intermediates and kinetic inertness of some compounds. Therefore, several reactions require the use of expensive organometallic reagents, toxic catalysts, or harsh reaction conditions, such as high temperatures and pressures, in addition to problems related to low selectivity or excessive generation of waste and byproducts. These limitations have been the principal challenge for organic chemists, especially in fine and pharmaceutical industries, which is to reduce the amount of waste generated in their operational systems.[3] Therefore, incorporation of green chemistry principles[4,5] has become an alternative in organic synthesis, leading to the development of more environmentally friendly methods, allowing the generation of complex molecules in a sustainable way.[6]

In this context, new techniques and strategies have been developed to solve sustainable problems, promoting selective and energy efficient chemical transformations, while minimizing the environmental impact of use of hazardous and toxic reagents, fossil solvents, and harsh conditions.[3,7] At this point, techniques such as electrochemistry and photochemistry, that use alternative catalytic approaches and unconventional energy sources, emerge as tools to promote synthetic efficiency, innovation, and sustainability in modern organic synthesis.[8,9]

1.1 Photochemistry

Over the past 15 years, the resurgence of photochemistry, particularly visible-light photocatalysis, has provided a powerful alternative. By using catalytic amounts of a photocatalyst capable of absorbing longer-wavelength light and transferring its energy or electrons to a substrate, reactive intermediates can be generated under mild conditions. This strategy enables cleaner reactions, improved selectivity, and higher yields.[10,11]

According to the International Union of Pure and Applied Chemistry (IUPAC), photochemistry is the branch of chemistry that studies the effects of light (from ultraviolet to infrared) on matter. Light-absorbing species

may be substrates, intermediates, or photocatalysts (chromophores). When the substrate itself is directly excited, the process is termed direct photochemistry. Because most organic molecules absorb in the UV region rather than in visible light, high-energy irradiation is often required, which can promote undesired side reactions and reduce selectivity.[12]

The processes occurring between light absorption and emission are described by the Jablonski diagram,[13,14] which outlines photophysical events that precede or accompany photochemical transformations. Excited states may decay radiatively *via* fluorescence ($S_1 \rightarrow S_0$) or phosphorescence ($T_1 \rightarrow S_0$) or non-radiatively through internal conversion or intersystem crossing (ISC). ISC ($S_1 \rightarrow T_1$) generates a triplet state, typically longer-lived than singlet states. Because phosphorescence and ISC are spin-forbidden processes, they are slower, increasing the probability that the triplet state participates in bimolecular reactions such as single-electron transfer (SET) or energy transfer (EnT).[15,16]

In photoredox catalysis, the excited photocatalyst can behave as either a strong oxidant or reductant, depending on its redox potentials.[17] In the oxidative quenching, the excited photocatalyst transfers an electron to the substrate, forming a reduced substrate and an oxidized photocatalyst, which is later regenerated by an electron donor. In the reductive quenching, the excited photocatalyst accepts an electron from the substrate, oxidizing it and forming a reduced photocatalyst, which is subsequently regenerated by an electron acceptor.[18]

SET processes may also occur without a photocatalyst *via* Electron Donor–Acceptor (EDA) or charge-transfer (CT) complexes. These arise from association between an electron-rich donor and an electron-poor acceptor, due to a bathochromic shift. Upon irradiation at the CT band, the excited complex generates a radical-ion pair within the solvent cage. Alternatively, excitation of one partner can lead to exciplex formation, which may also evolve into radical-ion intermediates.[19] EnT is a photophysical process in which a photosensitizer in its excited triplet state transfers energy (*via* Dexter or Förster mechanisms) to a substrate, promoting it to its triplet state. The excited substrate can then engage in radical transformations. Although the term “photosensitizer” is typically used in EnT catalysis, many photocatalysts can operate through both SET and EnT pathways.[20] HAT occurs when an electrophilic radical abstracts a hydrogen atom from a donor (usually at an electron-rich C–H position), generating a new radical and a stronger X–H bond. The newly formed bond generally has a higher bond dissociation energy (BDE) than the cleaved bond, driving the process thermodynamically.[21]

In summary, modern visible-light photocatalysis provides a sustainable and versatile platform for generating reactive radical intermediates under mild conditions. By harnessing controlled light–matter interactions and well-defined photophysical principles, it enables selective, efficient, and environmentally compatible synthetic transformations.

1.2 Electrochemistry

Electrochemistry is an alternative tool for altering the oxidation states of organic molecules, allowing the formation of new bonds, and has gained considerable attention in recent decades for its environmental benefits and synthetic efficiency.[22,23,24,25,26] Furthermore, it is a technique that allows transformations with selectivity, atom economy, and is environmentally friendly, producing minimal waste, with cost-effective.[27,28]

Organic electrosynthesis uses electrical energy to apply potential between a pair of electrodes, a cathode and an anode, in a solution containing the substrates. Organic molecules can be activated with the addition or removal of electrons. In the reduction process, it occurs at the cathode, and the molecule gains an electron at the LUMO, while for oxidation, which occurs at the anode, involves the removal of an electron from the HOMO of the molecule. These processes, occurring at the electrode surface, led to the formation of reactive intermediates, that generate radicals or charged molecules, allowing different reaction pathways, such as functionalization, activation, coupling reactions, and many others.[9,23-25]

One of the fundamental parameters in controlling these transformations is the applied electric current, the magnitude of which is adjusted according to the specificities of each protocol. In the context of organic electrosynthesis, the definition of this parameter aims to establish the ideal balance between reaction kinetics and selectivity. Although lower currents result in slower responses, they minimize the chances of competing pathways. Conversely, high currents provide an overpotential that can produce unwanted parallel reactions or manipulation of the medium. Furthermore, many of the green solvents involved in this review exhibit high viscosity and low dielectric constant. These properties significantly limited ionic mobility and mass transport, making the careful choice of current and the use of electrolytes (or cosolvents) crucial factors for system efficiency.

Therefore, electrochemistry has been a powerful tool for formation and activation of chemical bonds, like C-H,[29,30] C-N,[31,32] and C-C,[33] in addition to enabling the development of modern approaches in catalysis. However, in the last decade, only few examples have emerged of the application of somewhat unconventional bio-based solvents as a medium for these reactions.

1.3 Bio-based solvents: contextualization and applications in organic synthesis

Historically, the chemical industry has heavily relied on solvents derived from non-renewable fossil resources, many of which pose significant risks to human health and the environment due to their toxicity, volatility, and persistence.[34] With increasing pressure from governments and civil society to adopt more sustainable chemical practices, environmental regulations have become progressively stricter, particularly regarding the use of volatile organic compounds (VOCs), especially halogenated and aromatic solvents. In this context, the principles of green chemistry have played a pivotal role in promoting safer and more sustainable alternatives, as well as in redesigning chemical processes.[35]

Green solvents are central to this transition, particularly because industrial chemical operations, especially those related to pharmaceutical organic synthesis, consume large volumes of solvents. Consequently, replacing hazardous solvents with alternatives that exhibit improved environmental, health, and safety (EHS) profiles is highly desirable. Solvents derived from renewable resources, such as starch-rich feedstocks and lignocellulosic biomass, have gained considerable attention for their potential to reduce the environmental footprint of chemical manufacturing while maintaining process efficiency.[36] Bio-based solvents are typically produced from plant-based raw materials through chemical or biotechnological routes that are generally considered safer and more environmentally benign. Their advantages often include reduced VOC emissions, enhanced biodegradability, lower toxicity, and improved occupational safety.[37] Numerous studies have demonstrated that bio-based solvents can deliver satisfactory technical performance, indicating that sustainability gains can be achieved without compromising process efficiency.[38]

Despite these advantages, significant challenges remain, including optimizing production processes to improve cost competitiveness, selectivity, recyclability, and overall yield.[34] For large-scale and sustainable implementation, solvent production must be environmentally compatible and supported by carefully selected raw materials, considering factors such as availability, seasonality, physicochemical properties, accessibility, recyclability, and synthetic feasibility. Maintaining performance comparable to that of conventional solvents remains a central objective in solvent design and selection.[39]

Therefore, the transition from conventional fossil-based solvents to green, bio-based, and low-toxicity alternatives reflects a broader commitment to sustainable development within the chemical industry. This shift seeks to balance environmental protection, human health, economic viability, and technological performance in alignment with the principles of green chemistry. Bio-based solvents have been applied, for example, in different catalytic methods.[40,41] Considering the widespread use of ethanol and ethyl acetate, this review

surveys studies reported in the last five years in the fields of photo- and electrochemistry that employ less common bio-based solvents. In addition, the mechanistic aspects of the reported transformations are discussed.

2. Photochemical Reactions Promoted by Bio-based Solvents

2.1. 2-Methyltetrahydrofuran

2-Methyltetrahydrofuran (2-MeTHF) is obtained from two precursors, furfural and levulinic acid, with origins from hemicellulose and cellulose. Some of its physicochemical properties, such as miscibility with water, boiling point (80 °C), viscosity (0.6 cP at 25 °C), and stability to acids and bases, demonstrate that is a good alternative to solvents such as tetrahydrofuran (THF), dichloromethane (DCM), and chloroform ($CHCl_3$).[42] Furthermore, it is an alternative for procedures involving organometallics and organocatalysis, and exhibits excellent efficiency in biphasic reactions.[43-46]

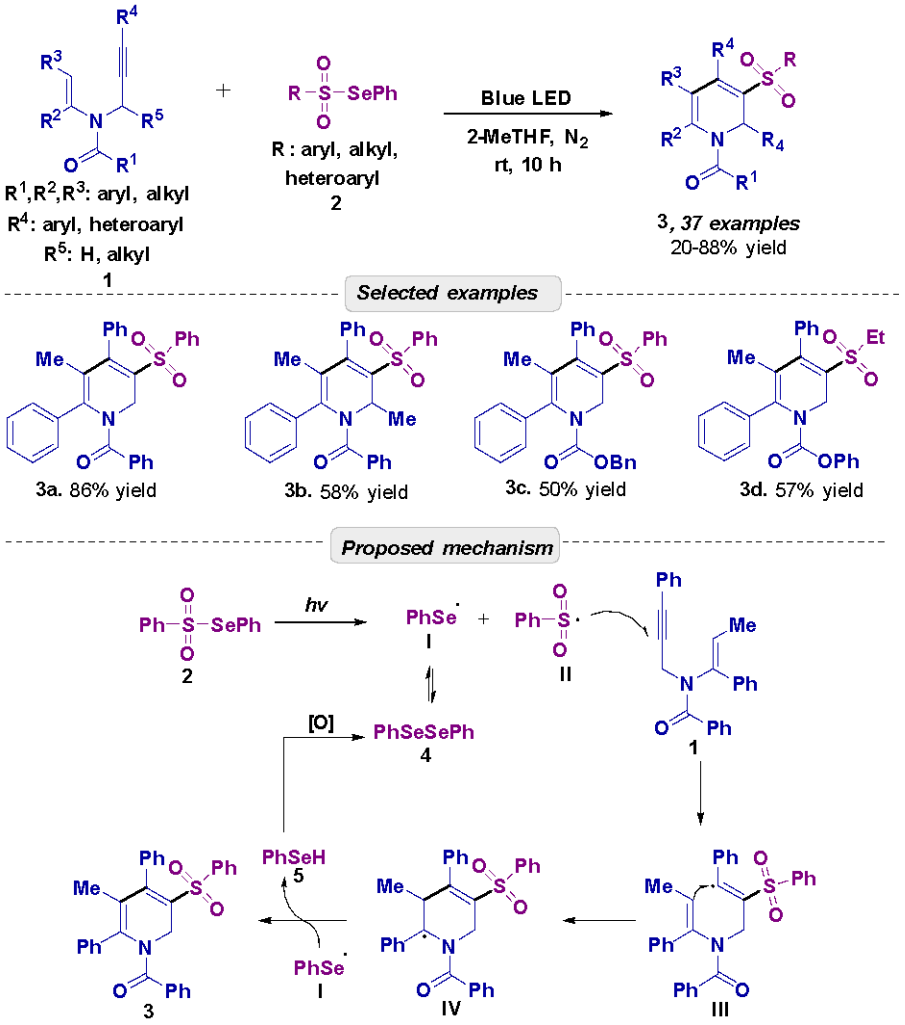

Scheme 1. Sulfonylation-cyclization protocol for the synthesis of functionalized 1,2-dihydropyridines **3**.

Concerning the photochemical processes, Xu et al. obtained pyridines and 1,2-dihydropyridines from *N*-propargyl enamides **1** and selenossulfonates **2** using a visible light-assisted protocol (30 W blue LED for 10 h), free of photocatalysts, additives and oxidants (Scheme 1).[47] During the optimization, different solvents were

studied, such as THF and DMF, to obtain the substituted pyridines, but 2-MeTHF proved to be the optimal solvent, affording a wide range of substituted pyridines in yields of up to 88%. Drawing on control experiments and established literature, the authors proposed a mechanism for the synthesis of **3**. The process begins with the light-induced homolytic cleavage of **2**, followed by the addition of the benzenesulfonyl radical to **1**. The resulting intermediate then undergoes a 6-*endo*-trig cyclization to form **IV**. Finally, the phenylselenyl radical is regenerated, prompting hydrogen abstraction from **IV** to afford the desired product.

Singh and coll.[48] developed a series of sulfonamides (**8**) using a transition metal-free and photocatalyst-free approach. The synthesis used various anilines **7** and sulfonyl chlorides **6** as starting materials and during the optimization phase, a variety of solvents were tested, including DMF, DMSO, DMC, H_2O and MeCN (Scheme 2). Although MeCN demonstrated to be effective, providing the desired product in 82% yield, further investigation identified 2-MeTHF as a better alternative, achieving 86% yield. This solvent was therefore adopted for the synthesis of the target sulfonamides **8**. Regarding the mechanism, the authors conducted an UV-visible absorption study and observed a bathochromic shift, which may be indicative of an electron donor-acceptor complex (EDA) pathway for the reaction progress. Thus, they proposed that a complex is formed between **6** and **7**, which, followed by a single electron transfer (SET) furnishing radicals **I** and **II**, that upon combination produced intermediate **III**, which is deprotonated, generating the desired sulfonamide **8**.

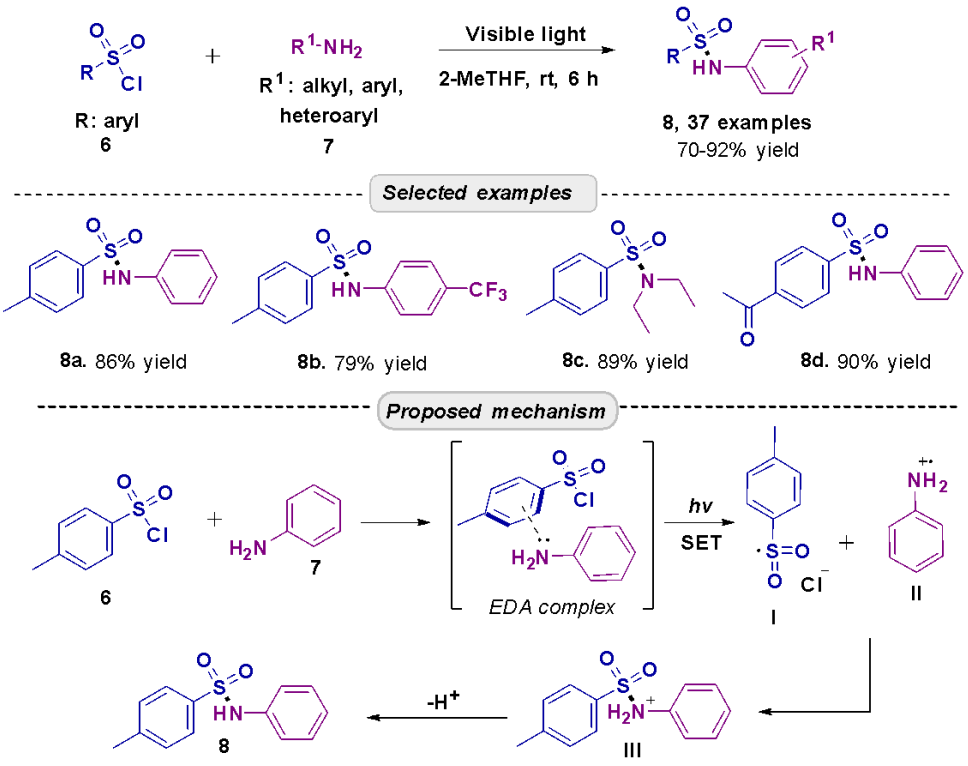

Scheme 2. Visible light assisted synthesis of sulfonamides **8**.

Meng et al.[49] developed a synthetic strategy involving sulfonylation followed by cyclization of 1,6-enynes **9** with sulfonyl chlorides **6** under visible light irradiation. During the optimization process, the authors evaluated various solvents, including THF and EtOAc. Since the latter performed poorly, likely due to the low solubility of the reactants, 2-MeTHF emerged as the most effective solvent enabling the synthesis of a variety of lactams in moderate to high yields (Scheme 3). The authors proposed a mechanism based on the formation of the sulfonyl

radical **II**, which is obtained through the cleavage of **6**. This radical then adds to the 1,6-enyne, yielding a vinyl species **IV**, that subsequently undergoes hydrogen abstraction to afford the desired product **10**.

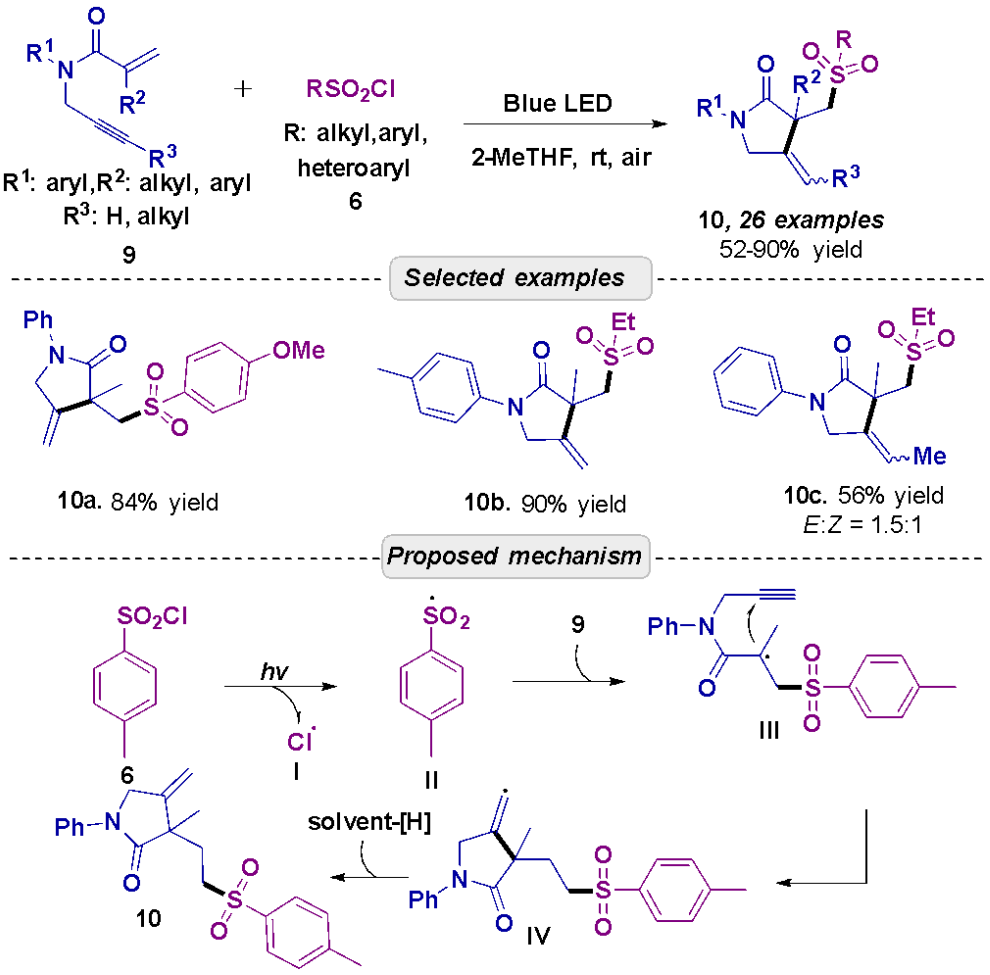

Scheme 3. Regioselective sulfonylation/cyclization of 1,6-enynes **9** with sulfonyl chlorides **6**.

Heterogeneous photocatalysis for the synthesis of thiophosphates **13** was explored by Zhan and coll.[50] (Scheme 4). They developed a lead-free bismuth-based perovskite, such as cesium bismuth bromide ($Cs_3Bi_2Br_9$) type photocatalyst to facilitate the oxidative dehydrogenative coupling between thiols **12** and phosphoryl compounds **11** in 2-MeTHF. Notably, this reaction proved efficient even in the absence of acid or base additives. The catalyst demonstrated robust stability and was successfully recycled for subsequent runs without significant loss of activity. Other solvents were also evaluated, such as DMF, MeCN, 1,4-dioxane, DMSO, DCM, EtOAc, acetone, DMC and various alcohols (MeOH, EtOH, and ^{i}PrOH), albeit lower yields were obtained. The authors proposed that the process initiates with charge separation on the photocatalyst surface, generating electron (e^-) and hole (h^+) carriers. These electrons activate molecular oxygen to form superoxide radicals, which are subsequently oxidized by the holes to produce singlet oxygen ($^1O_2$). Notably, $^1O_2$ abstracting a proton to generate the thiyl radical, this species then undergoes homocoupling to yield disulfide **14**. Concurrently, the phosphorus-centered radical is generated from the P(O)H precursor, either through a direct oxidation process or SET pathway. Finally, this phosphorus radical couples with thiyl radical (path a) or reacts with disulfide (path b) to afford the target compound.

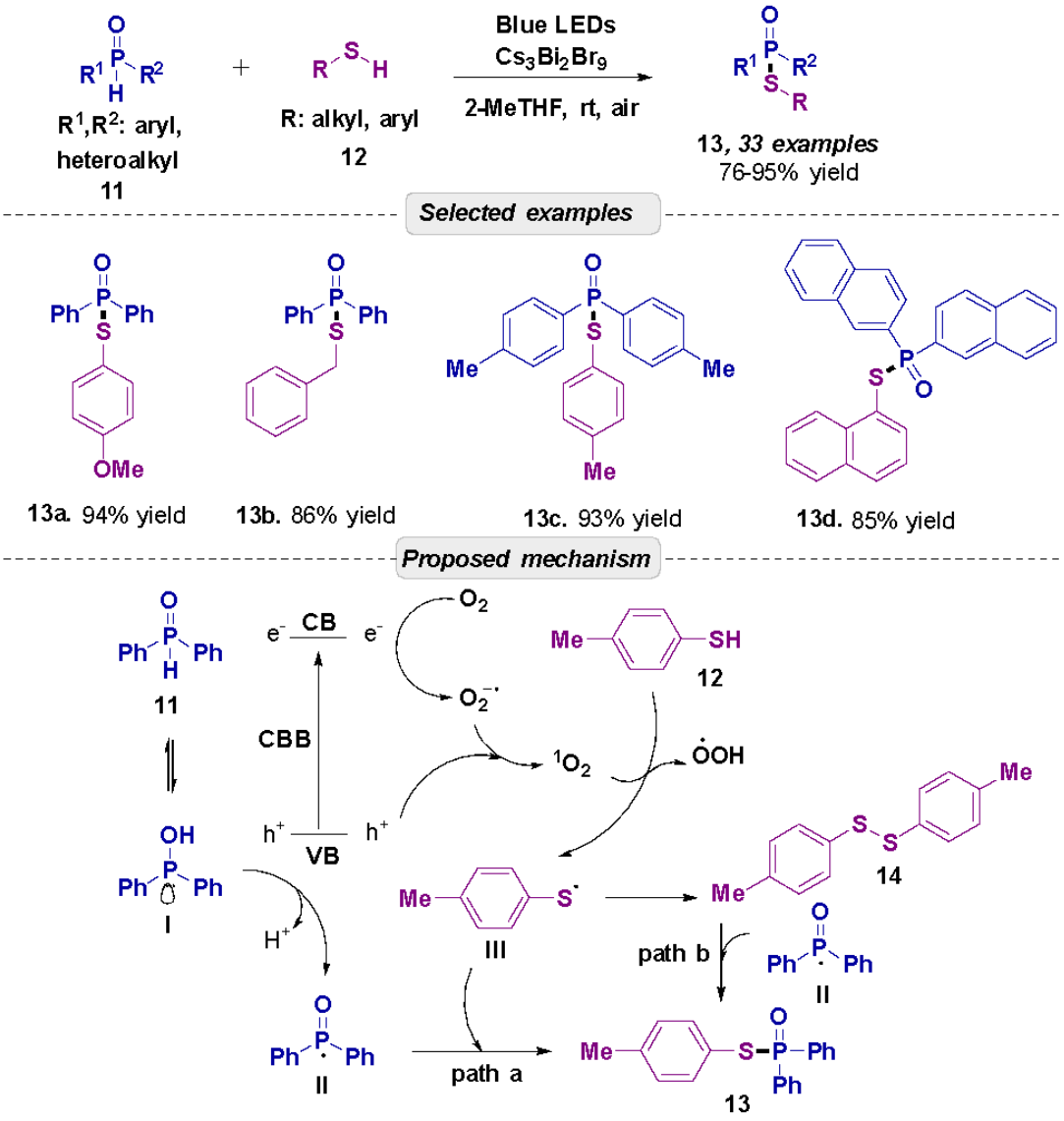

Scheme 4. Heterogeneous photocatalysis-mediated synthesis of thiophosphates **13**.

Difluoromethylated oxindoles **17** were also synthesized using visible light in 2-MeTHF.[51] This photocatalyst-free approach employed *N*-methyl-*N*-phenylmethacrylamides (**15**), diacetoxyiodobenzene [$PhI(OAc)_2$] and CHF_2CO_2H **16** as difluoromethylating agents. Although other solvents, such as THF, MeCN, toluene, acetone, EtOAc and DCM were evaluated, they resulted in lower yields. Under the optimized conditions, the protocol provided access to a scope of 26 difluoromethylated oxindoles with yields reaching 96% (Scheme 5). The proposed mechanism for the synthesis of these *N*-heterocycles begins with an exchange of functional groups between **16** and $PhI(OAc)_2$, generating species **18**. Upon excitation by the light source, this intermediate produces **I** and **II**. The resulting CHF_2 radical then attacks substrate **15** to form the carbon-centered radical **III**, which undergoes a SET to yield cation **IV**. Finally, deprotonation of **IV** promoted by the difluoroacetate anion affords the desired oxindoles while regenerating CHF_2CO_2H.

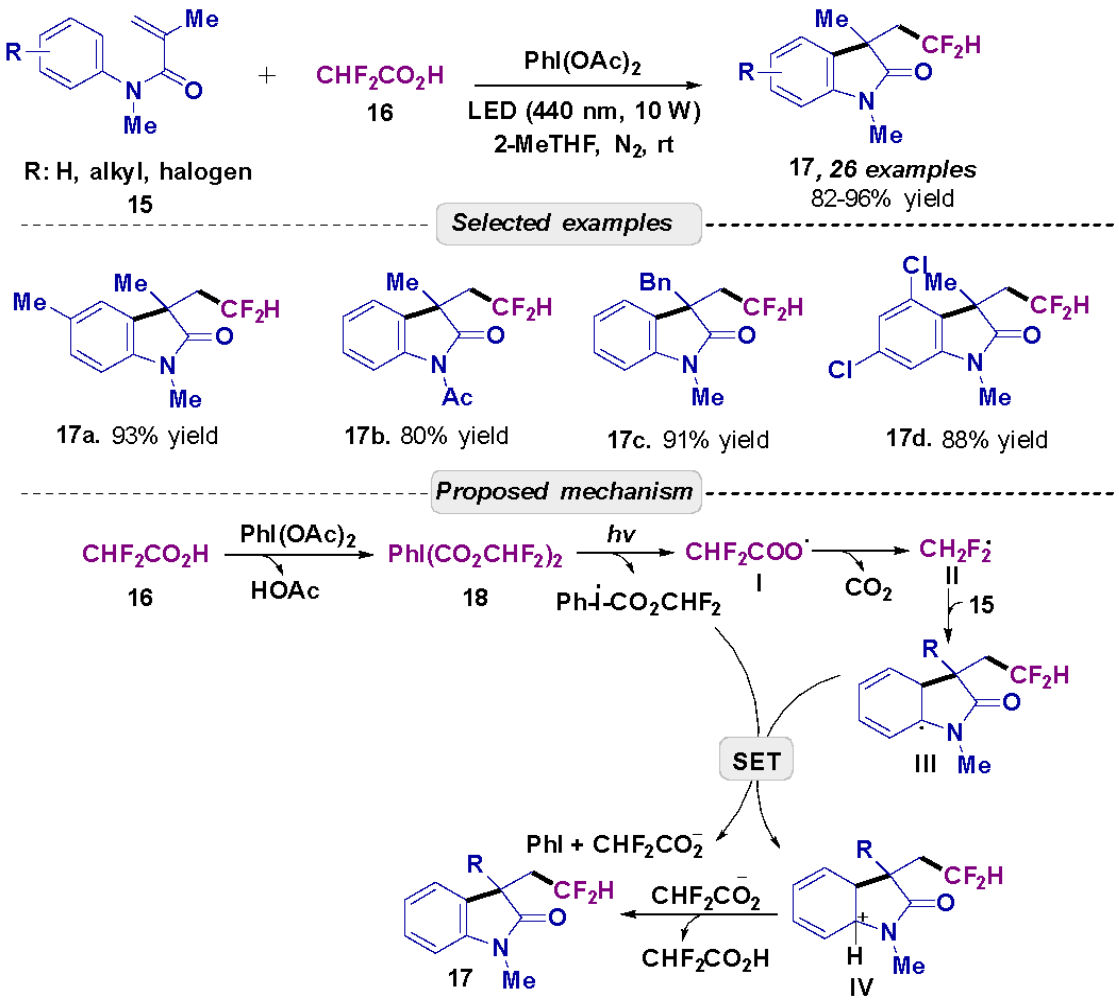

Scheme 5. Synthesis of difluoromethylated oxindoles **17**.

Fused indoles were synthesized *via* a catalyst-, base-, and acid-free photoinduced strategy (Scheme 6).[52] The protocol is based on sulfonylation followed by cyclization to obtain the fused diazepinone **21**. Different solvents were evaluated, as DMSO, EtOAc and MeCN, that led to the formation of the desired product with good yields over a period of 12 h. However, when THF and 2-MeTHF were tested, the reaction was faster (2 h) with excellent yields, so the latter was chosen to continue the studies. The developed protocol allowed the obtaining of a wide scope consisting of fused indole derivatives with yields of up to 93% (Scheme 6). UV-vis absorption studies did not detect any bathochromic shift, which is evidence that EDA complexes are not involved in this process. Thus, it was proposed that **20** initially undergoes homolysis when absorbing light, forming the sulfonyl radical **I** and a seleno radical **II**. Subsequently, the sulfonyl radical **I** is added to **19**, causing the formation of **III**. Next, oxidation of **IV** with the seleno radical **II** occurs, resulting in the loss of a proton, leading to the desired product **21**.

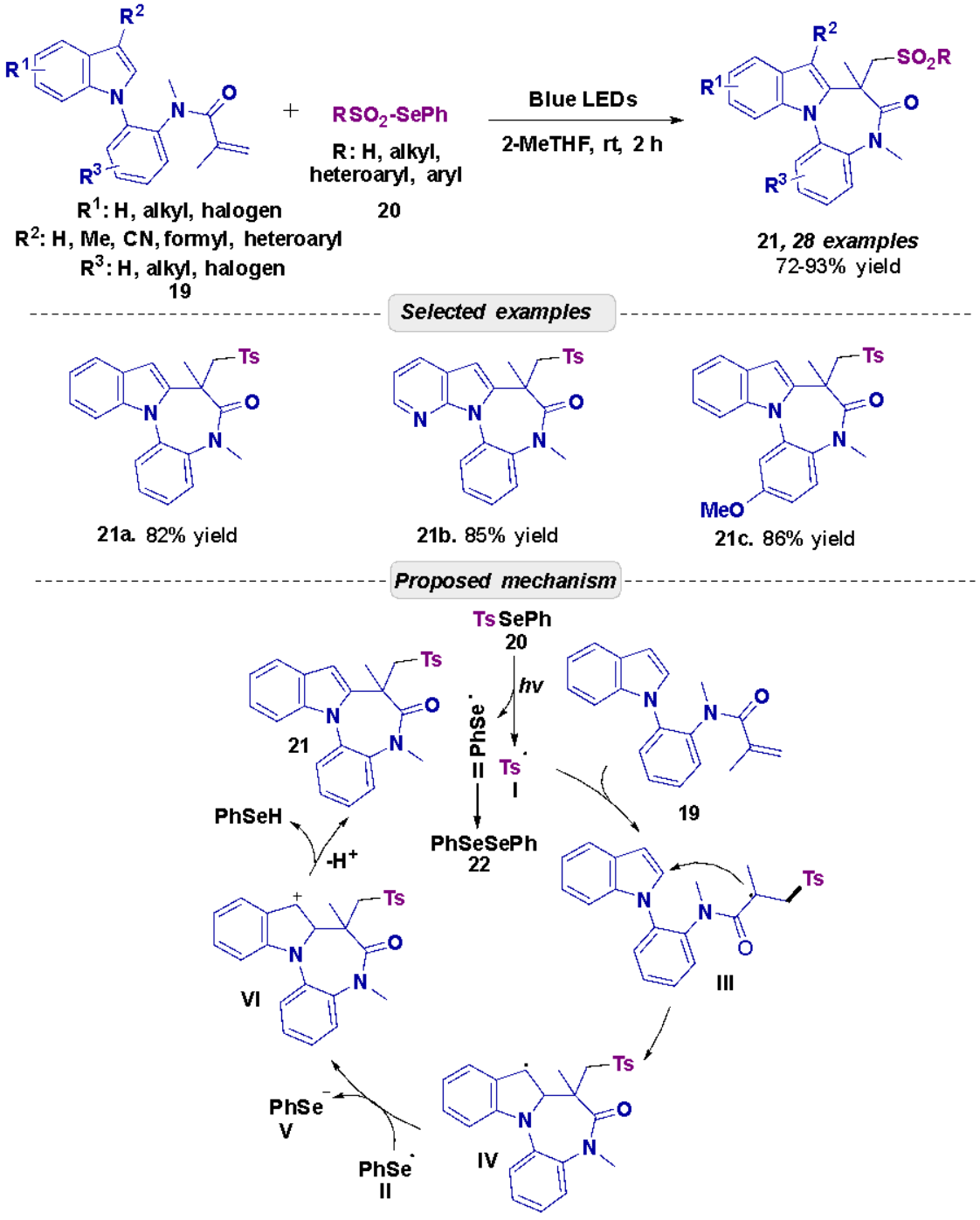

Scheme 6. Photoinduced synthesis of indole-fused **21**.

Functionalized dihydrobenzofurans **24** were obtained through a photochemical strategy based on 1,5-hydrogen transfer followed by cyclization between 2-alkynyl ethers **23** and sulfonyl chlorides **6** (Scheme 7).[53] This protocol did not employ photocatalysts or additives to aid the progress of the reaction. During the solvents screening, EtOAc, for example, did not favor the obtaining of the desired product, then THF and 2-MeTHF were evalulated, with the latter being adopted to continue the studies. The developed protocol allowed the synthesis of 26 dihydrobenzofuran derivatives with yields of up to 93%. For a better understanding of the mechanism, UV-vis studies were conducted and revealed that the transformation studied does not proceed through an EDA complex. Thus, **6** was brought to its excited state by light absorption. Subsequently, the sulfonyl radical inserts

itself into the alkyne **23**, promoting the formation of alkenyl **25**, that through an intramolecular 1,5-HAT, **III** was formed. This intermediate undergoes a 5-*exo*-trig cyclization, promoting conversion to the intermediate **IV**, that abstracts a hydrogen from the solvent (2-MeTHF), forming the dihydrobenzofuran of interest **24** (Scheme 7).

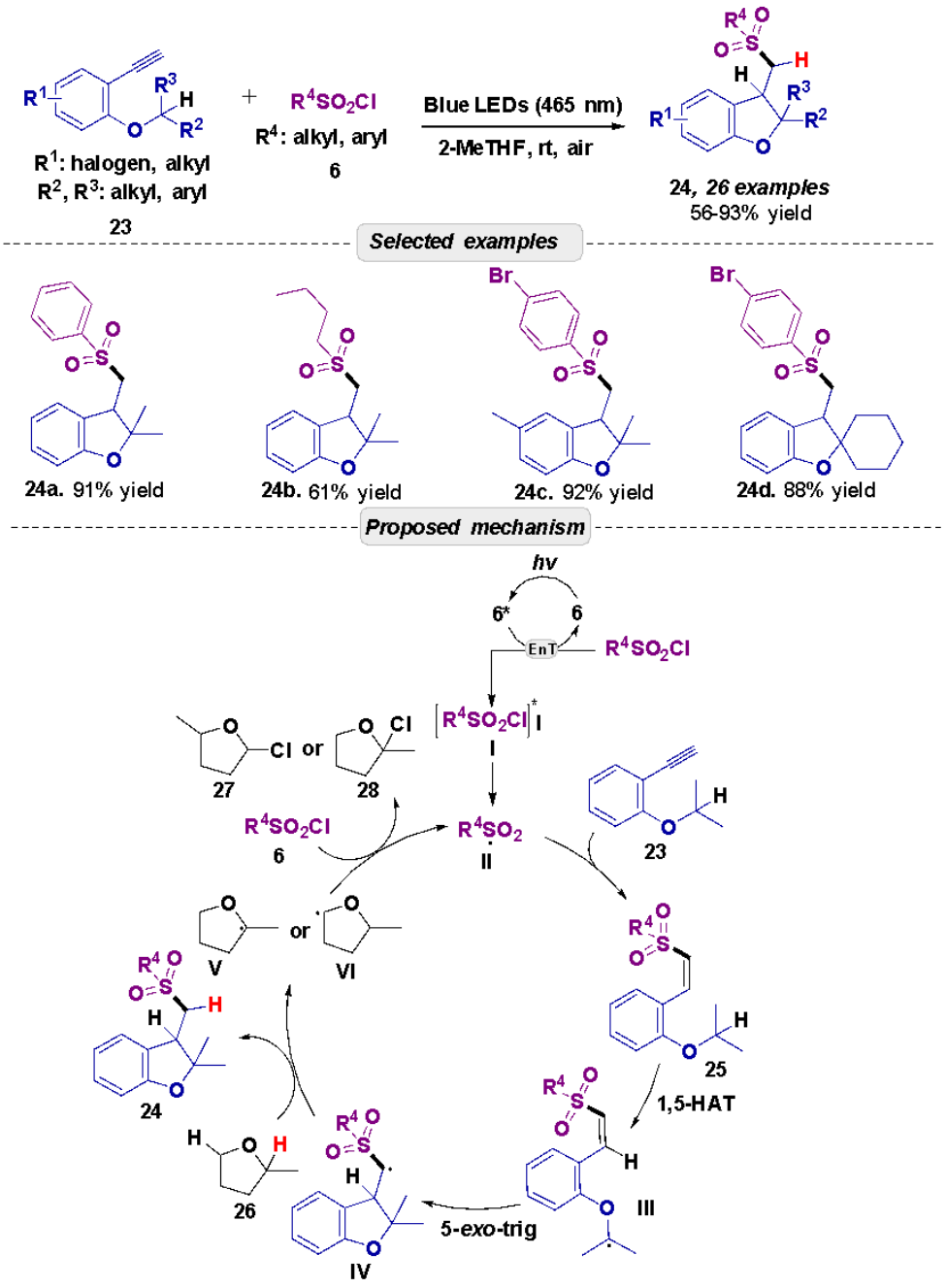

Scheme 7. Synthesis of functionalized dihydrobenzofurans **24** promoted by visible light.

3,3'-Disubstituted oxindoles **31** were obtained by Lu et al.[54] using a photoinduced coupling of indolin-2-ones **29** and β-sulfanil esters **30** *via* 1,2-sulfur translocation (Scheme 8). The method proceeded under mild conditions, allowing for a broad reaction scope consisting of more than 50 examples of 3,3'-disubstituted oxindoles. Different solvents were explored, such as THF, DCM and MeCN, which allowed the desired product to be obtained with good yields, although still lower than 2-MeTHF. Based on UV-vis studies, the authors proposed that the reaction proceeds *via* the EDA complex. This complex formed between enolate **I** and **30**,

triggering a SET process that produces the radicals **II** and **III**. After the fragmentation of **III**, the alkene **32** and the thiol radical **IV** are generated. Finally, a radical-radical coupling between the benzyl species **V** and the oxindole provides the desired product (Scheme 8).

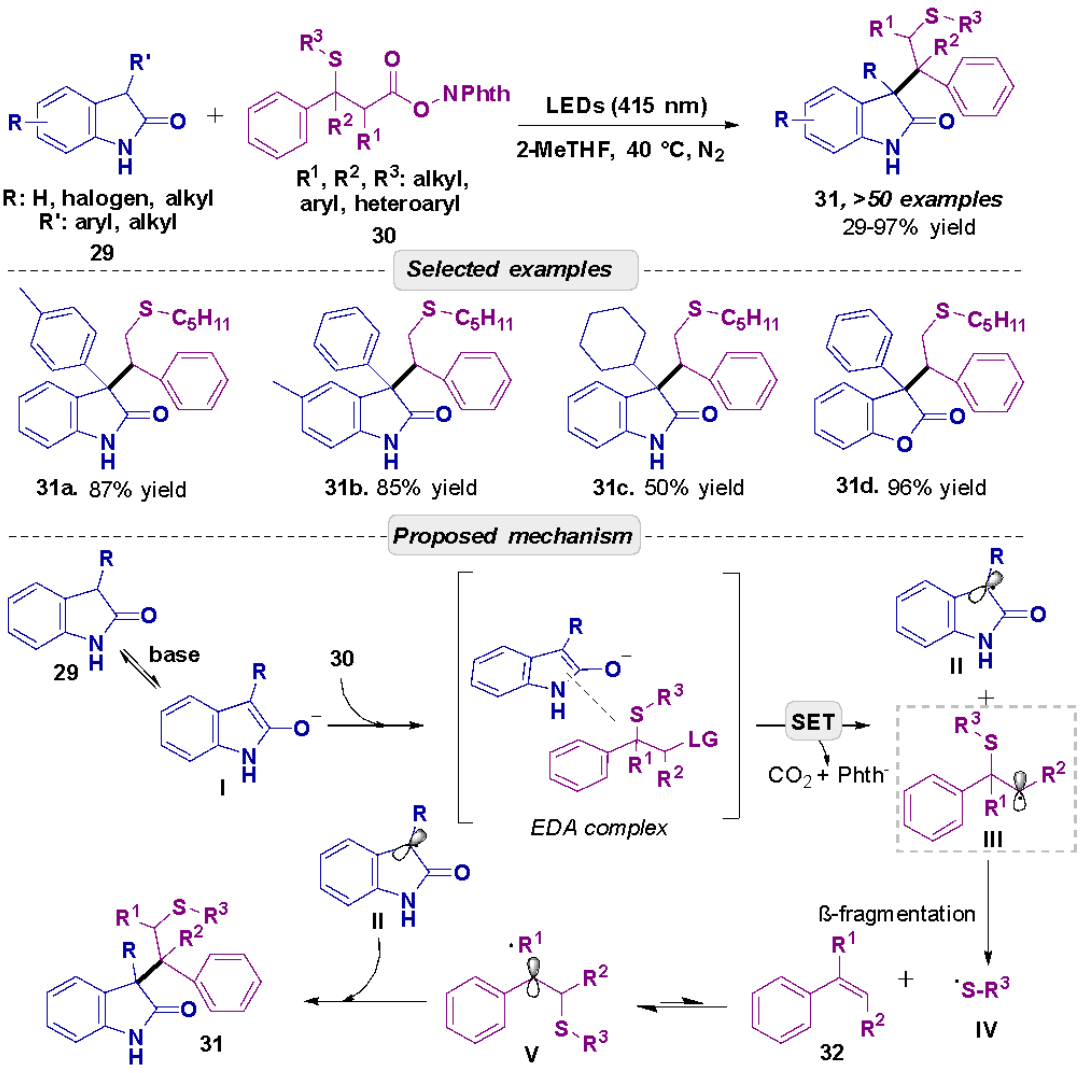

Scheme 8. Construction of 3,3′-disubstituted oxindoles **31** *via* a photochemical process.

Xiao et al. reported the synthesis of β[2,2,3]-amino esters through a visible-light-mediated radical-radical coupling protocol, driven by chiral phosphoric acid (CPA) catalysis.[55] The method utilized β-keto esters **33** and *N*-acetyl α-amino acid-derived esters **34** in the presence of 1,2,3,5-tetrakis(carbazol-9-yl)-4,6-dicyanobenzene (4CzIPN) (**35**) as photocatalyst. Throughout the optimization study, different solvents were screened, including CH_2Cl_2, CH_3CN, EtOAc and THF, and ultimately, 2-MeTHF delivered the best enantioselectivity and was chosen as the optimal solvent (Scheme 9). The authors conducted several control experiments, such as radical trapping, luminescence quenching experiments, cyclic voltammetry, and EPR studies. Based on the evidence gathered and reports from the literature, the mechanism was proposed. The process likely begins with the formation of a hydrogen-bonded complex between ester **III** and the chiral catalyst, facilitating enolization. Within the photoredox cycle, this complex undergoes SET with the excited state [4CzIPN]* generating the radical anion $[4CzIPN]^{\bullet-}$. Subsequently, the reduced photocatalyst transfers an electron to the NHPI ester, triggering decarboxylation to yield the α-amino-alkyl radical **II**, alongside phthalimide and CO_2.This step closes the catalytic

cycle, leading to a radical-radical coupling. This coupling is steered by a chiral environment, maintained through double hydrogen-bonding interactions with the CPA catalyst **37**.

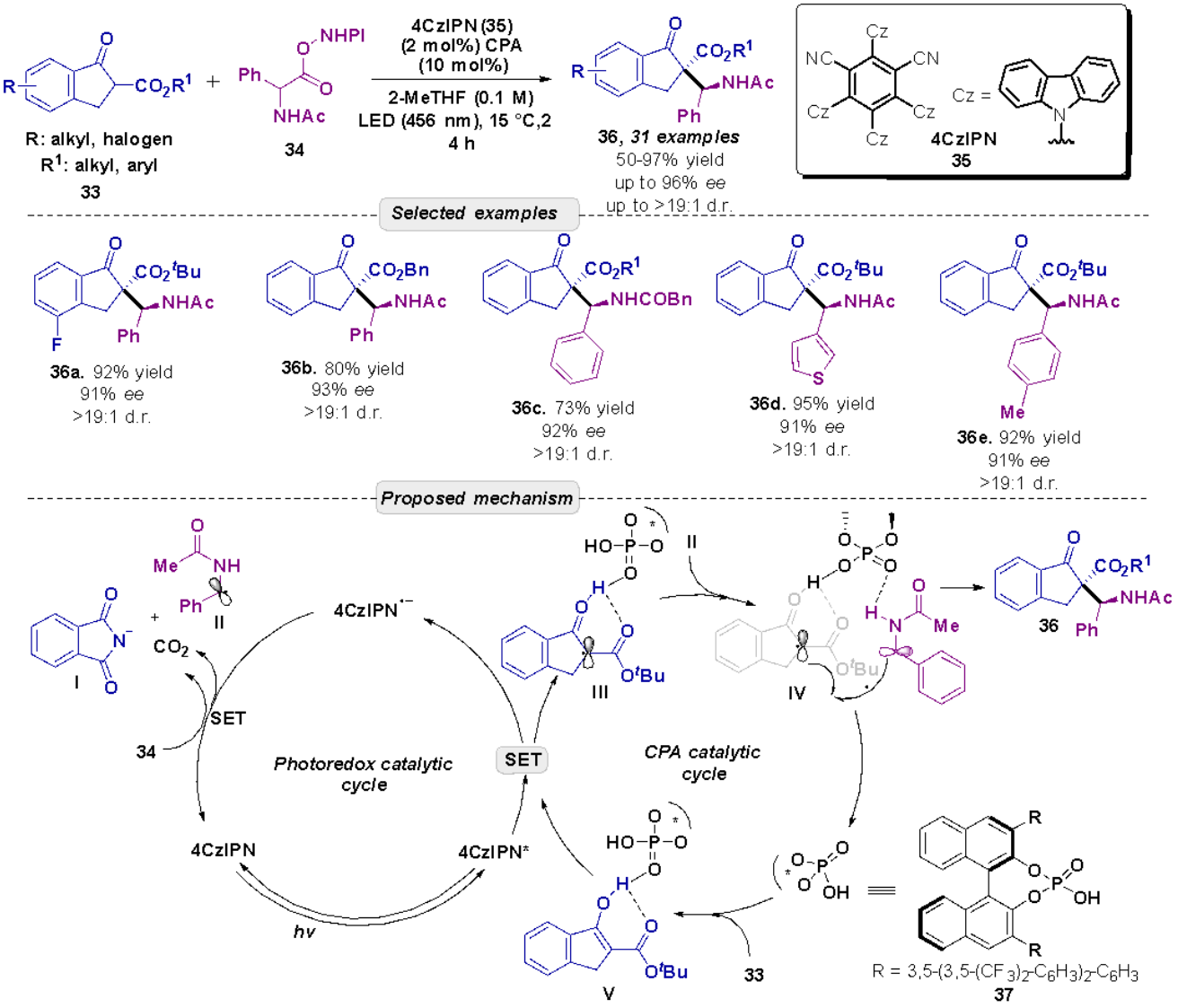

Scheme 9. Synthesis of β[2,2,3]-amino acid esters conducted by enantioselective radical coupling.

The He's group developed a series of quinazolinones with fused phosphorylated rings *via* heterojunction approach using the heterogeneous photocatalyst V_2O_5/g-C_3N_4 (Scheme 10).[56] The model reaction was established between quinazolin-4(3*H*)-one (**38**) and diphenylphosphine oxide (**11**). An initial screening of solvents (including EtOAc, EtOH, DMC, H_2O, acetone, MeCN, DMF, and DMSO) proved challenging, yielding the desired fused quinazolinone only in modest amounts (up to 25% yield). Although several of these common solvents showed low reactivity, switching to THF and 2-MeTHF significantly increased the conversion, yielding derivative **39** with yields of 51 and 83%, respectively. Taking advantage of these optimized conditions, the scope was expanded to 37 derivatives, achieving yields of up to 83%. The proposed mechanism proceeds via a SET process, where electrons react with molecular oxygen to generate the superoxide radical anion. Simultaneously, holes (h^+) in the valence band (VB) of V_2O_5 oxidize the phosphinic acid **I**, generating a radical cation **II** that undergoes deprotonation to yield the phosphinoyl radical **III**. This reactive species then attacks the substituted

quinazolinone **38**, forming an intermediate radical which undergoes subsequent cyclization. In the final stages $O_2^{\cdot-}$ abstracts an electron from the cyclic intermediate to produce a cation **VI**; subsequent dehydrogenation and aromatization then afford the desired fused compound.

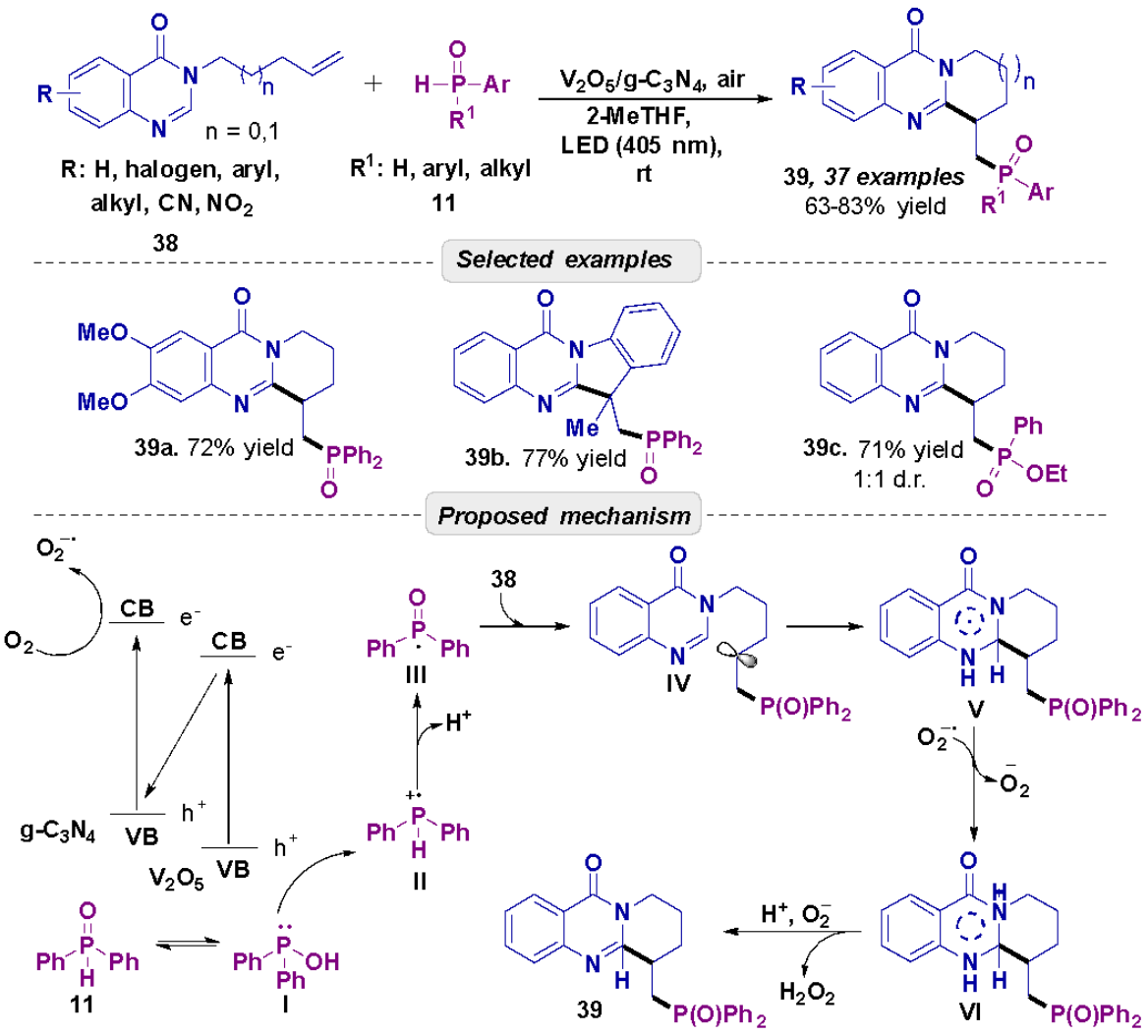

Scheme 10. Protocol for obtaining quinazolinones **39**.

A dual catalytic strategy was explored for the thioesterification process, leveraging a synergistic nickel and organophotoredox manifold (Scheme 11).[57] The protocol utilized aryl, heteroaryl, and vinyl iodides alongside potassium thioacetate derivatives **41** as coupling partners. During the optimization study, several solvents—including CH_3CN, DMF, dioxane, and cyclopentyl methyl ether (CPME)—were evaluated. However, these consistently resulted in lower efficiency compared to 2-MeTHF, which was ultimately selected as the optimal medium. This method enabled the synthesis of 32 compounds, with yields reaching up to 99%. The proposed mechanism begins with the photoexcitation of the photocatalyst to its excited state. Potassium thioacetate **41** is then oxidized by [4CzIPN]***via* SET to generate a thiocarboxylate radical **II**. Simultaneously, the nickel cycle is initiated: the Ni^{2+} precursor can undergo reduction to a lower valence species or participate in a ligand exchange with the thiocarboxylate anion. This is followed by oxidative addition or radical capture to form a Ni^{2+}-sulfide intermediate, which is subsequently modulated by SET steps. Finally, the nickel complex undergoes oxidative addition to the aryl halide **40**, followed by reductive elimination to produce the desired thioester **43**.

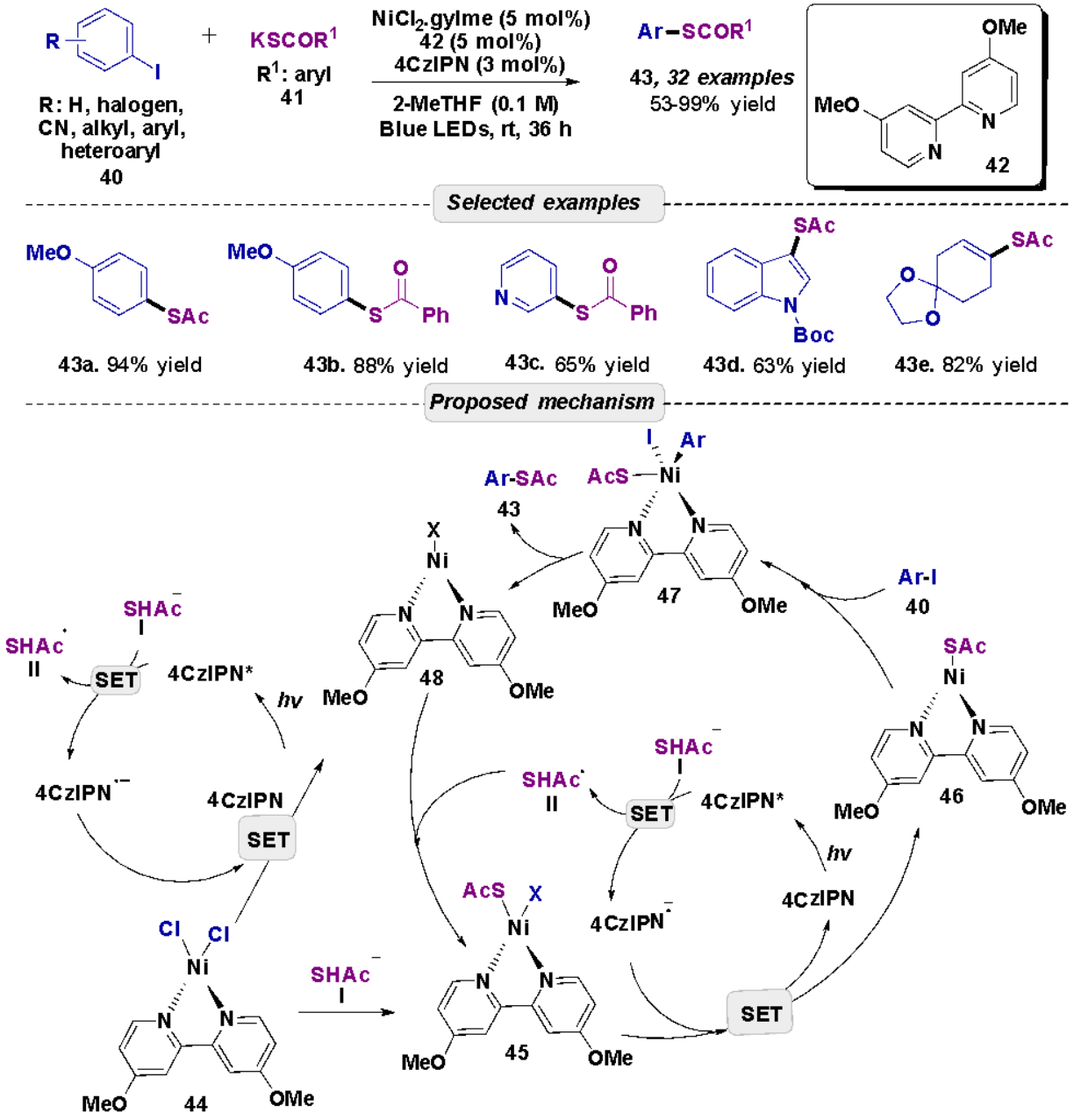

Scheme 11. Visible light-mediated thioesterification.

The Greaney's group evaluated the arylation of 2-arylpyridines **50** using aryl bromides and iodides **49**, catalyzed by $[RuCl_2(p\text{-cymene})]_2$ in the presence of KOAc (Scheme 12).[58] This protocol yielded both mono- and di-*ortho*-arylated products **51** and **52**. During the additive screening, most carboxylates and amino acids failed to improve the reaction, with the exception of an acetylisoleucine derivative, which was then selected for further studies. While various solvents were tested as alternatives to 2-MeTHF—including MeOH, DCM, MeCN, and DMF—none showed better results. Ultimately, this approach provided 36 examples with yields reaching up to 81%.

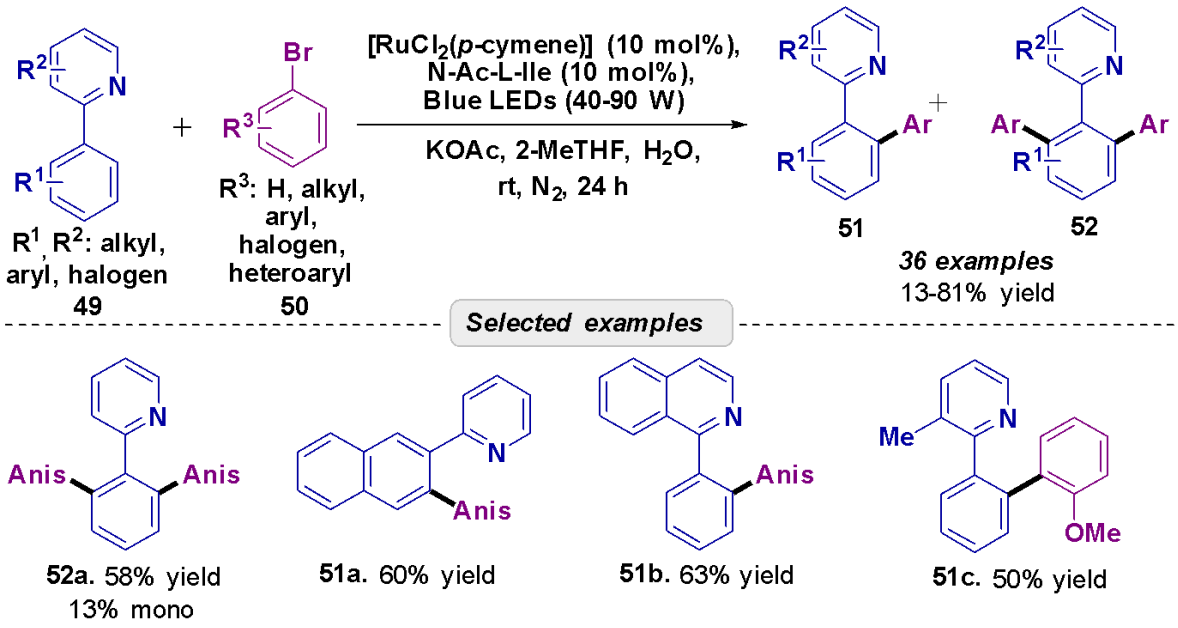

Scheme 12. Ruthenium-catalyzed *ortho*-arylation of heterocycles under visible light irradiation.

Heterogeneous photocatalysis was explored as a fluoroalkylation strategy (Scheme 13).[59] In this context, the material Yb@g-C_3N_4 was employed as a photocatalyst, and two isocyanides **53** and RSO_2Cl **6** species were explored as starting materials under ultrasound irradiation (US). Other homogeneous photocatalysts were evaluated (*fac*-[Ir(ppy)$_3$], Ru(bpy)$_3$Cl$_2$, rhodamine B, 4CzIPN), however, they did not present satisfactory conversion. Regarding the solvent screening, besides 2-MeTHF, with MeCN, EtOH, and *N*,*N*-dimethylacetamide (DMA) the yields were lower. However, when using DCE, the yield for obtaining **54** was higher when compared to 2-MeTHF, but even so, it was selected as the best solvent, as it made the protocol more environmentally friendly. It is worth noting that the Yb@g-C_3N_4 was recovered and reused and remained effective for up to eight recycling cycles. The authors proposed a mechanism initiated by the light-driven excitation of the heterogeneous photocatalyst, generating e^- and h^+ pairs in the conduction (CB) and valence (VB) bands. Following this, Yb^{3+} captures an electron to form the transient Yb^{2+} state, which subsequently reduces the RSO_2Cl species *via* SET. This process yields a radical anion that, after the rapid extrusion of Cl^- and SO_2 generates the radical **II**. This radical then adds to the isocyanide **53** to produce an imidoyl intermediate **III**, which undergoes intramolecular cyclization. Finally, the desired compound **54** is obtained through a HAT step.

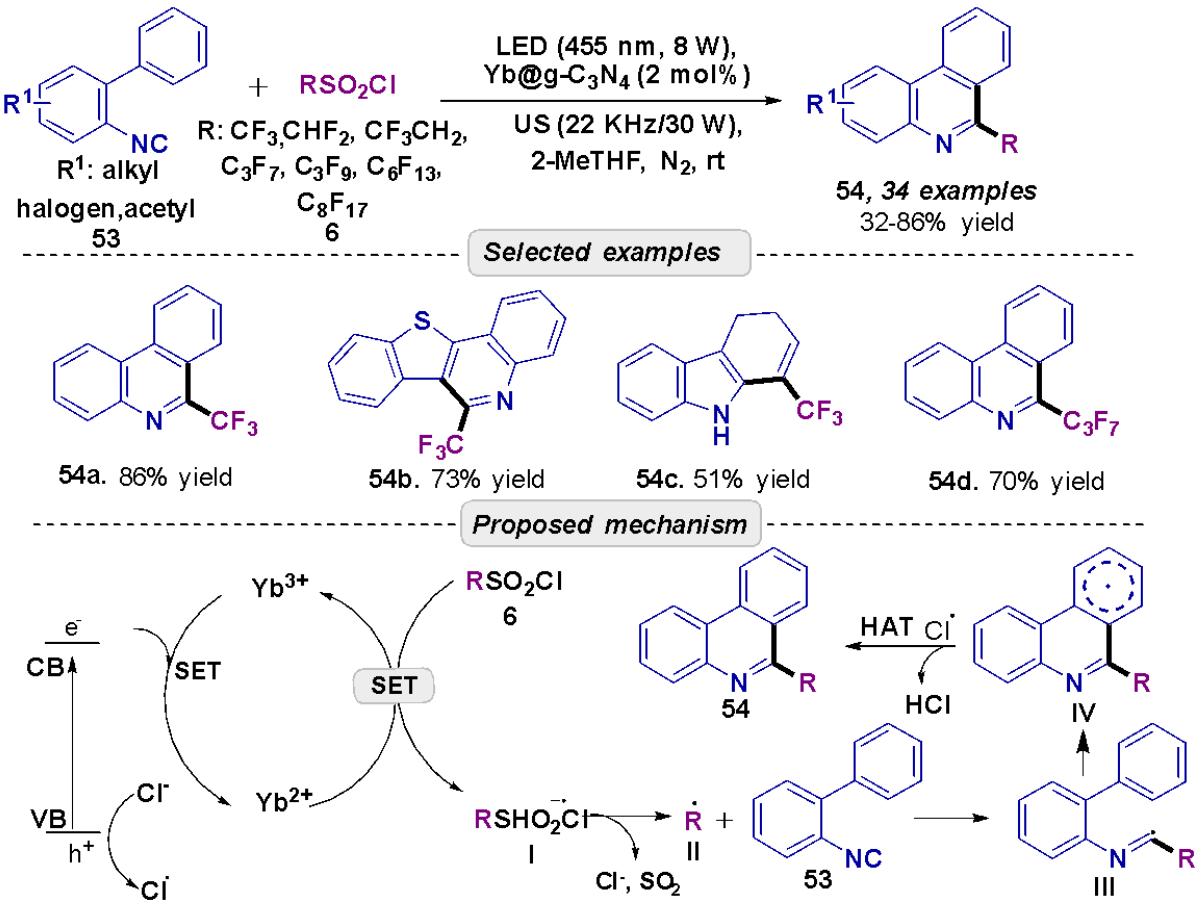

Scheme 13. Heterogeneous photocatalysis-mediated fluoroalkylation strategy.

Sun and coll. investigated a Minisci-type reaction through a semi-heterogeneous enantioselective catalytic approach, using quinoline **55** and racemic *N*-acetylphenylalanine-derivative **56** as starting substrates (Scheme 14).[60] The study employed mesoporous graphitic carbon nitride (mpg-CN) as photocatalyst, which proved robust enough to remain active for up to 10 cycles. While 2-MeTHF was the primary solvent used, the authors also explored 1,3-dioxane; however, this alternative led to a lower yield of the target compound and a noticeable decrease in enantiomeric excess (*ee*). The authors conducted control studies and proposed a reaction mechanism based on previous literature. In this pathway, the heterogeneous photocatalyst performs a SET on the radical precursor **34** to generate the α-aminoalkyl radical **I**. Once the protonated heterocycle is incorporated into the cycle, it yields **III**, which then undergoes deprotonation to afford the desired product **58** or **59**.

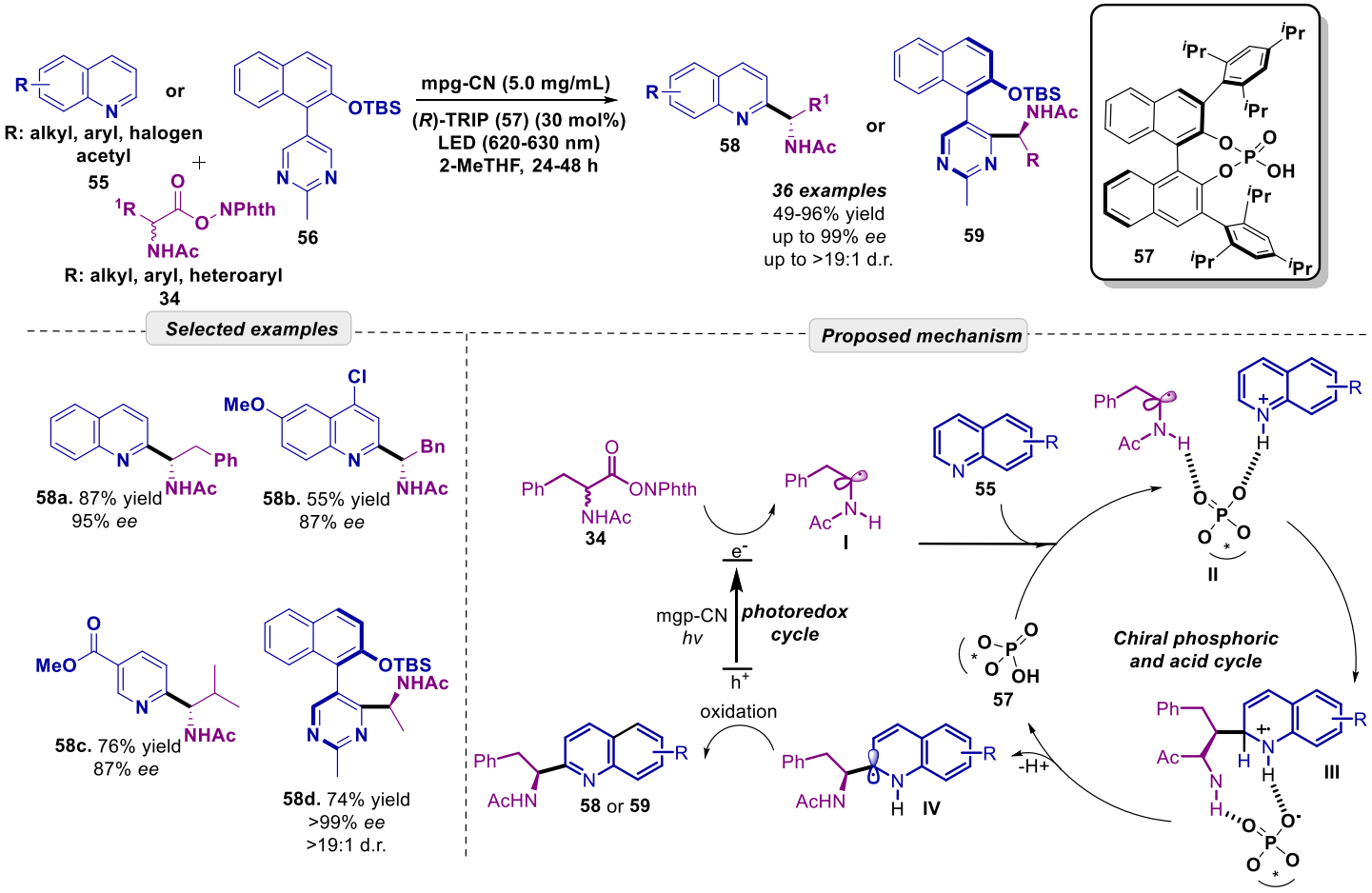

Scheme 14. Enantioselective Minisci-type reaction mediated by red light.

The Kokotos' group has developed several photochemical aerobic oxidation strategies for sulfides, in the absence of a catalyst, utilizing irradiation at 370 nm with 2-Me-THF as the bio-based solvent.[61] Additionally, two distinct processes were evaluated using anthraquinone (AQ) **61**—under either a CFL lamp or 427 nm irradiation—also in 2-Me-THF. To demonstrate the practical utility of these methods, the authors applied them to the synthesis of active pharmaceutical ingredients (APIs), specifically sulforaphane and modafinil. Overall, this approach enabled the preparation of 26 different sulfides with yields reaching up to 99% (Scheme 15). Drawing on both their previous findings and existing literature, the authors proposed distinct catalytic cycles for these oxidations. The first pathway involves the generation of singlet oxygen in the presence of the photocatalyst (Scheme 15a), which then oxygenates the sulfide to form a persulfoxide intermediate. This intermediate subsequently reacts with a second sulfide molecule, yielding two equivalents of the desired sulfoxide. Alternatively, a second pathway proceeds *via* SET between the excited-state photocatalyst and the sulfide. This generates a sulfide radical cation, which, upon reacting with triplet oxygen, affords the target sulfoxide. In the catalyst-free process (Scheme 15b), singlet oxygen remains a key species. It is important to highlight that even in the absence of anthraquinone (AQ) **61**, the reaction still operates through the sulfide radical cation intermediate.

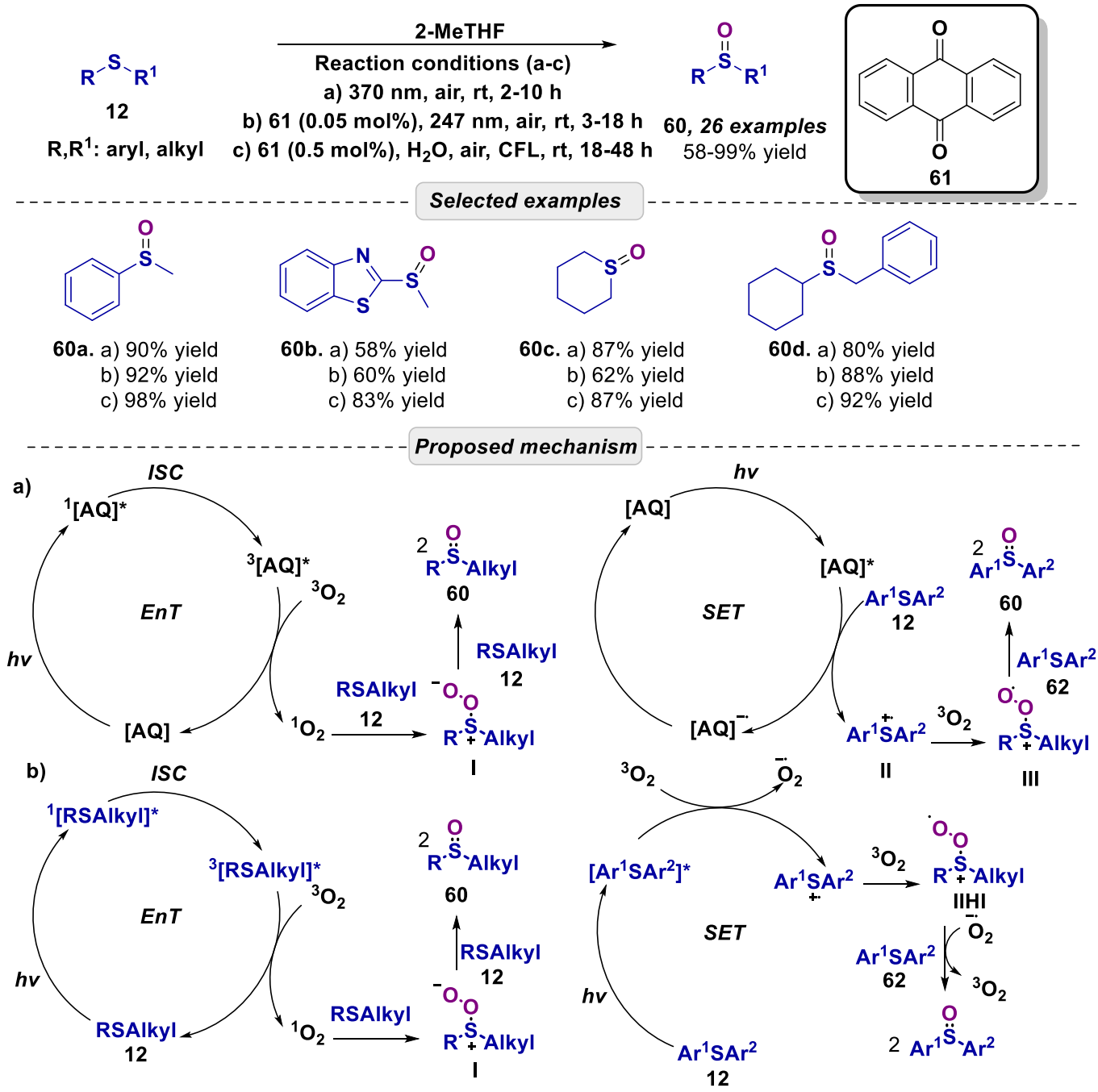

Scheme 15. Different aerobic sulfide oxidation strategies. Proposed mechanisms: a) anthraquinone-catalyzed and b) photocatalyst-free.

Zhang and coworkers described a visible light-induced [3+2] cycloaddition for the synthesis of pyrazoles and (spiro)-pyrazolines in the absence of a photocatalyst.[62] During the optimization of the method—using *N*-tosylhydrazone **63** and butyl acrylate **64** as model substrates—alternative solvents such as THF and MeCN were evaluated; however, 2-MeTHF consistently outperformed these media, yielding superior results. This robust strategy enabled the synthesis of a diverse library of over 50 compounds, with yields reaching up to 98% (Scheme 16). The authors proposed a mechanism that begins with the deprotonation of **63** to afford the corresponding *N*-tosylhydrazone anion. Under light irradiation, a non-covalent interaction between this anion

and DBU facilitates the formation of **II**. Subsequently, the diazo species **III**, generated *in situ*, undergoes a [3+2] cycloaddition with alkene **64**, ultimately yielding the target cycloadduct **65** or **66**.

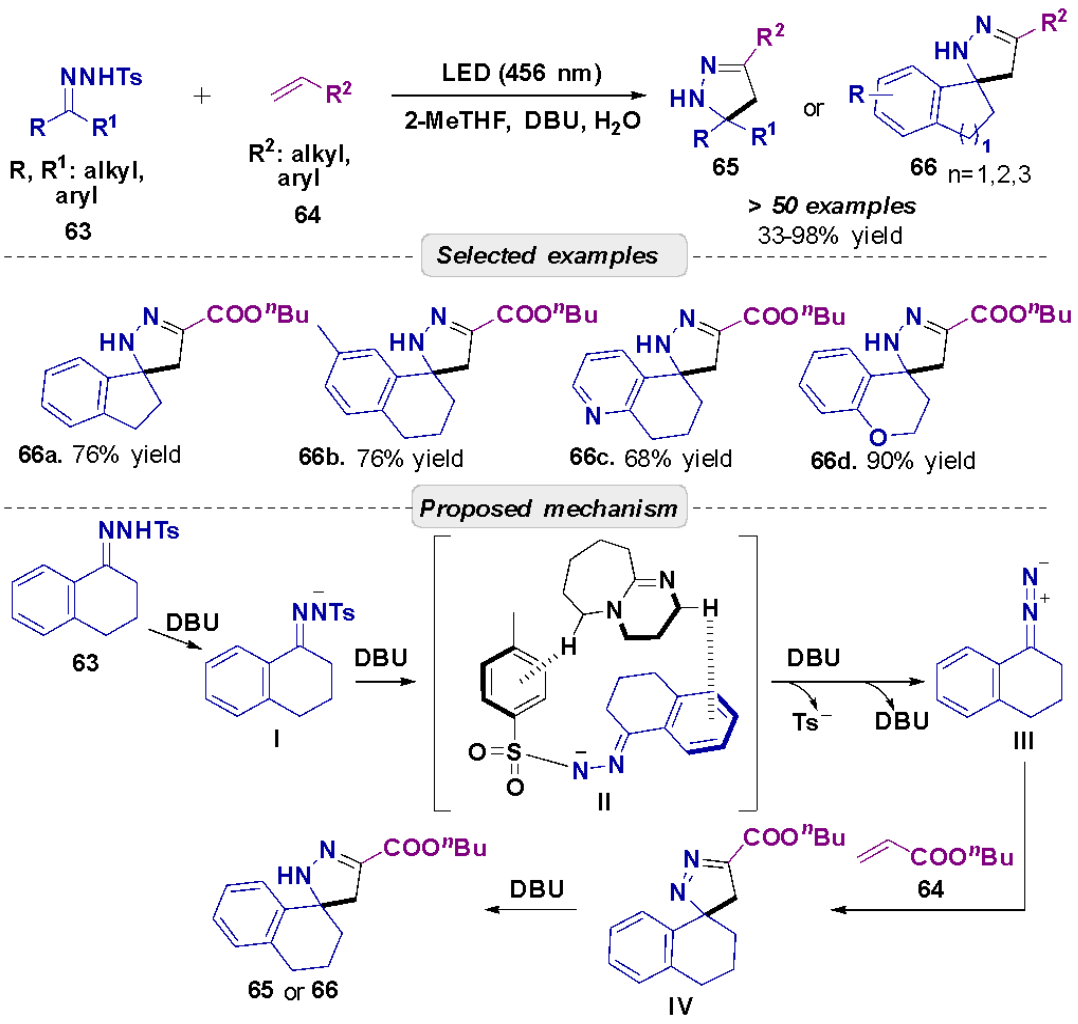

Scheme 16. Synthesis of (spiro)-pyrazolines and pyrazoles *via* [3 + 2] cycloaddition.

Zhu and coll. developed a catalyst-free, energy-transfer-driven strategy for the aryl heterofunctionalization of non-activated alkynes **67**, yielding polyfunctional olefins **68** (Scheme 17).[63] During the development of this protocol—initially employing *N*-(2-methylbut-3-yn-2-yl)-*N*-tosylacetamide **67** and tosyl chloride **6** as model substrates—the authors screened various traditional solvents, including THF, 1,4-dioxane, MeCN, DMF, and DCE. Interestingly, none of these media provided the target product. Success was only achieved upon evaluating THF, EtOH and 2-MeTHF, which the authors suggest may play a dual role as both the reaction medium and the essential hydrogen source. Notably, when expanding the substrate scope to include radical precursors such as vinyl selenides and vinyl sulfides, 2,2,2-Trifluoroethanol (TFE) was identified as the optimal solvent. The mechanism proposed by the authors begins with the reaction between the radical of interest and the terminal alkyne **67**, generating the alkenyl radical intermediate **II**. This species is then intercepted by the aryl group of the sulfonyl precursor, triggering a radical Smiles rearrangement. Following the extrusion of SO_2 the resulting carbon-centered radical abstracts a hydrogen atom from the solvent to yield the final product **68**.

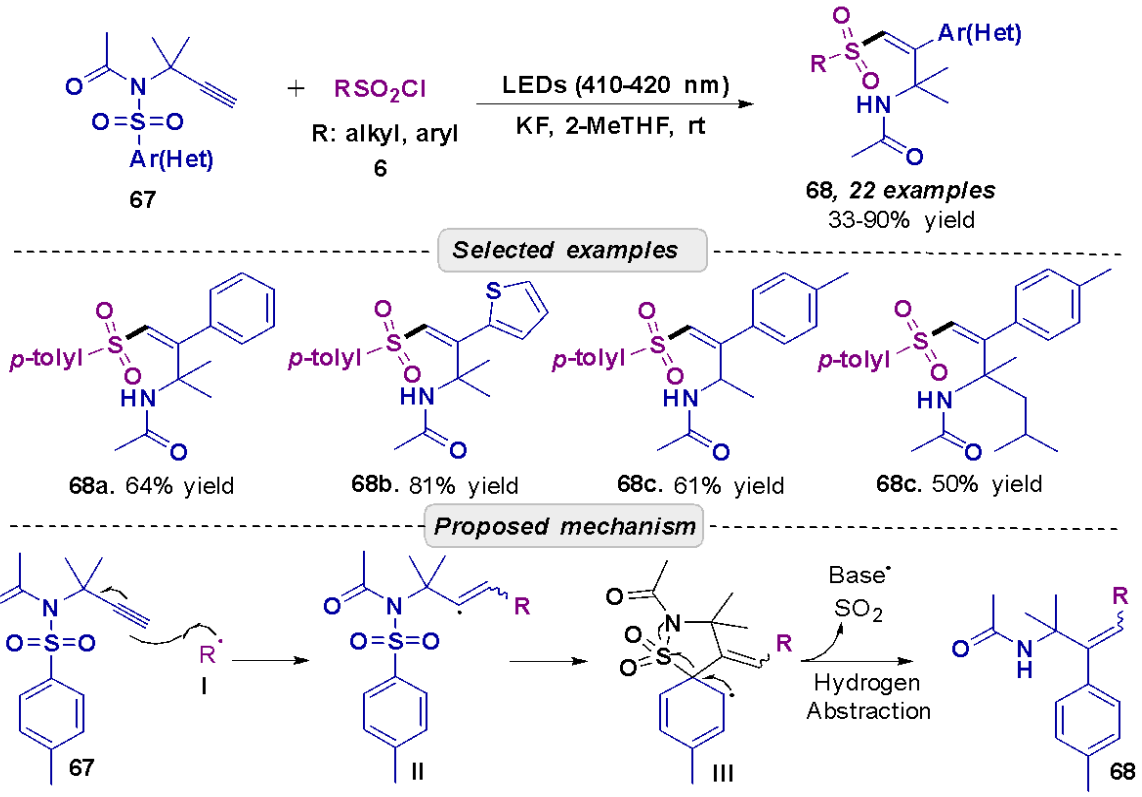

Scheme 17. Light-assisted stereoselective protocol for the synthesis of polyfunctional olefins.

Dai and coworkers developed a photoredox alkynylation protocol utilizing tertiary amines **70** and alkynyl bromides **69** to produce the corresponding propargylamines **72**.[64] Initial optimization identified $Ru(bpy)_3Cl_2$ as the photocatalyst, K_2PO_4 as the base, and MeOH as the solvent. However, these conditions proved unfavorable for tertiary aliphatic amines, yielding only trace amounts of the desired products. To address this limitation, a second optimization was conducted (Scheme 18), where 2-MeTHF was employed as a bio-based alternative solvent and [Ir(ppy)2(dtbbpy)]PF6 as catalyst. This adjustment significantly improved the outcome, enabling the synthesis of eight compounds with yields reaching up to 80%.

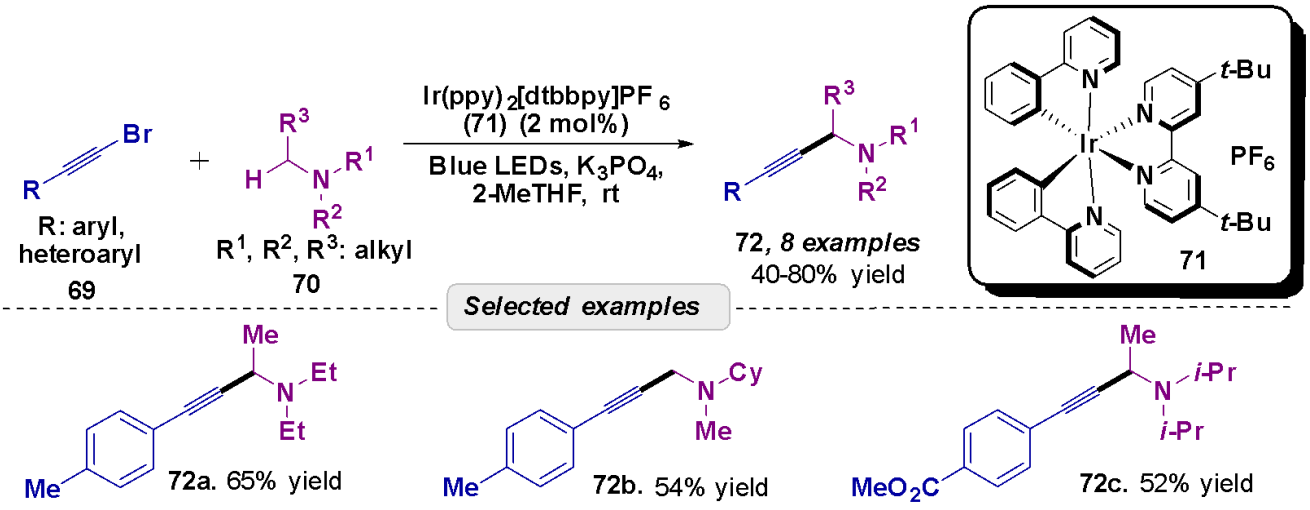

Scheme 18. Photoredox alkynylation strategy.

2.2 Ethyl Lactate

Ethyl Lactate (EL) is formed through the esterification between lactic acid and ethanol catalyzed by a strong acid. Some physicochemical properties made possible its use in organic synthesis, as for example, density (1.028 $g.cm^{-3}$ at 25 °C), boiling point (193 °C) and viscosity (4.7 cP), are similar to other usual solvents. Due to these properties, EL has the capacity to replace some conventional solvents, such as *N*-methylpyrrolidone, toluene, dichloromethane, and chloroform.[42,65,66] Furthermore, it is a non-toxic, non-corrosive, non-carcinogenic, and biodegradable solvent. With this, EL and its aqueous solutions have been studied in various organic synthesis methodologies, such as coupling reactions, metal-catalyzed reactions, multicomponent reactions non-covalent bonds activation.[67,40] It also has many industrial applications, such as in pharmaceuticals and cosmetics.[65]

In 2020, Zhang and coll.[68] explored photoredox reactions under visible light irradiation, demonstrating photocatalytic operations which can be conducted in renewable solvents without significant loss of yield or selectivity. Therefore, the synthesis of spirooxindole derivatives **77**, involving isatin **73**, ethyl acetoacetate **74**, and malononitrile **75** was performed at room temperature, with Na_2-eosin Y (**76**) as photocatalyst, and 10 W green LED (Scheme 19). The choice of EL was because during the optimization studies it afforded the best results when compared with other conventional solvents, such as $CHCl_3$, CH_3CN, THF, DMF, EtOAc and MeOH. Pure ethyl lactate provided 81% yield, but in aqueous solution a better yield was obtained, reaching 90% in proportions of 1:1 or 3:2 (EL/H_2O). The proposed mechanism begins with the tautomerization of malononitrile **75** in the presence of ethyl lactate, generating **78**. Next, Knoevenagel condensation of **78** with isatin **73** occurs, eliminating a water molecule and forming intermediate **79**. At this point, visible light applies additional energy to accelerate the reaction, as eosin Y can act as a catalyst for hydrogen atom transfer (HAT), activating the C-H bond and generating an *α*-carbonyl carbon radical **I**. This radical is captured by **79**, forming adduct **II**. Subsequently, reverse hydrogen atom transfer (RHAT) occurs between eosin Y and adduct **II**, regenerating the photocatalyst and forming intermediate **80**. Finally, **80** suffers intramolecular cyclization, forming the desired product **77**.

Using a similar approach, Mohamadpour *et al*. developed a visible light-mediated photocatalytic strategy for synthesis of spiroacenaphthylenes **86** and 1*H*-pyrazolo[1,2-*b*]phthalazine-5,10-diones **87** (Scheme 20).[69,70] The main objective of this study was to change the traditional methods based on metal catalysts, for a metal-free and sustainable method. In the study, the EL/H_2O (2:1) mixture afforded the best yield (93%), a higher value when compared to others conventional organic solvents, like $CHCl_3$, DMF, DMSO, MeCN, MeOH, EtOAc, EtOH and pure EL. The optimal reaction conditions used Na_2-eosin Y (1.5 mol%) as a photocatalyst, 18 W white LED at room temperature and air atmosphere. For the mechanistic study, the author suggests that photo-excited Na_2-eosin Y acts *via* HAT. After light absorption, eosin Y abstracts a hydrogen atom from the activated substrate, generating a radical intermediate, which participates in a Knoevenagel condensation followed by Michael addition, intramolecular cyclization and tautomerization.

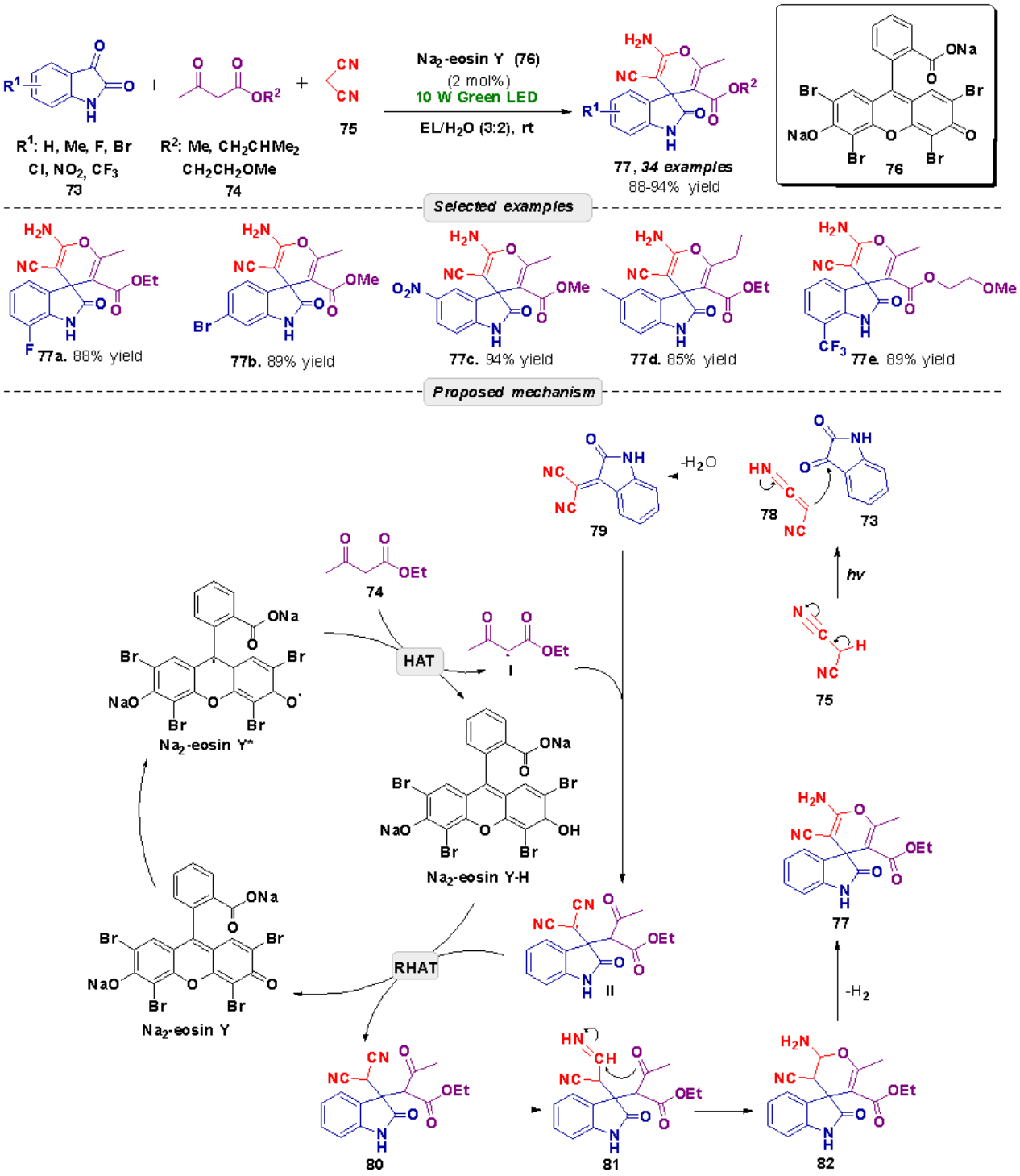

Scheme 19. Photochemical synthesis of spirooxindole **77** with EL.

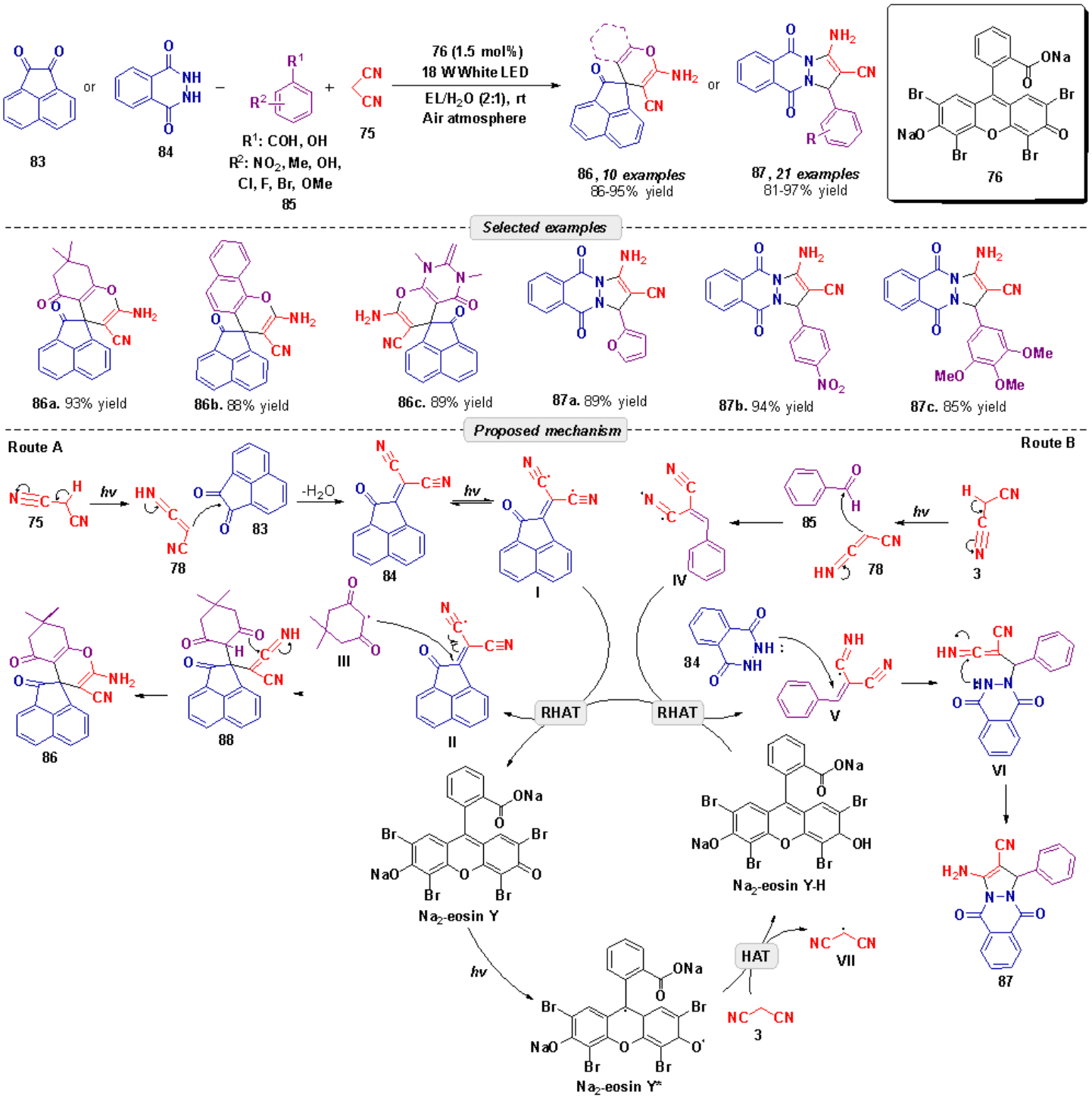

Scheme 20. Photochemical protocol for spiroacenaphthylenes and 1*H*-pyrazolo[1,2-*b*]phthalazine-5,10-diones.

3. Current Applications of Bio-based Solvents in Electrosynthesis

3.1 Cyrene

Dihydrolevoglucosenone (DLG or cyrene) is a dipolar aprotic solvent produced through the pyrolysis of cellulose **89** to produce levoglucosenone **90** followed by catalytic hydrogenation to the desired product **91** (Scheme 21).[71] It can be used as a substitute for more commonly used fossil solvents, like DMF, DMA and NMP, due to fact to

have some similar physicochemical properties, such polarity, dipolar moment, and boiling point.[42,72,73] Its molecular structure contains a ketone and an acetal, which can coordinate with reactive intermediates in the reaction medium. These interactions enable cyrene to stabilize the intermediates, such anionic radicals and ionic species, that may influence reaction pathways and selectivity in organic electrochemical reactions, making it particularly attractive for applications in electrosynthesis.[73]

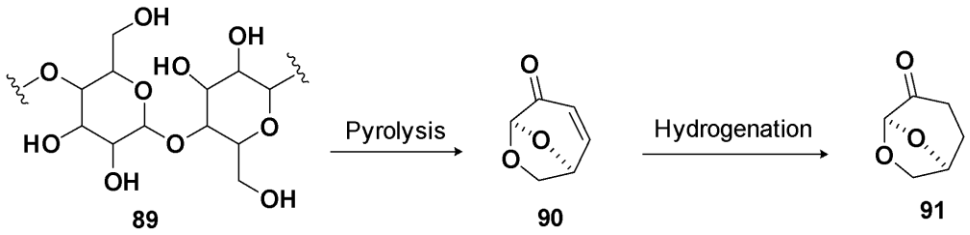

Scheme 21. General route to produce cyrene.

But the use of cyrene in electrosynthesis presents application challenges associated with its properties. This solvent has a high dielectric constant (37.3)[74] associated with a high viscosity (14.5 cP at 25 °C), considerably higher than other conventional aprotic dipolar solvents, like DMF (0.9 cP) and DMSO (1.99 cP).[70] The high viscosity results in low ionic mobility and high ohmic resistance in the electrochemical system, limiting charge transport. Even using a supporting electrolyte, the electrical conductivity remains low, requiring high salt concentrations to obtain acceptable values.[73,75] Because of this, it has energy dissipation and needs to apply a higher potential, generating an increased risk of side reactions. Thus, the use of cosolvents, such as ethanol or water, has been adopted to reduce the resistance of the medium, improving electrical conductivity, and enable applications of cyrene in electrosynthesis reactions.

In 2023, Ramos-Villaseñor and coworkers described the first application of cyrene as the main solvent in the electrochemical reduction of benzophenone (Scheme 22) [73] Because of the high viscosity and low conductivity of cyrene, the use of ethanol as a cosolvent was important to enable the reaction. In the presence of tetrabutylammonium tetrafluoroborate (Bu_4NBF_4) as a supporting electrolyte, the electrochemical reduction of benzophenones **92** occurs *via* two-electron transfer, leading to the corresponding alcohol **94**. The other components of this reaction are glassy carbon as working electrode and platinum as counter electrode, with 5mA/cm^2 as constant current. Different solvents were tested, such as DLG/water 1:2, DLG/MeOH 1:2, and EtOH, furnishing low yields, whereas a mixture of DLG/EtOH 1:1 ratio afforded the best result with 70% yield. For the reaction work-up, it was performed an extraction with ethyl acetate followed by treatment of the organic phase with aqueous KOH solution at 50 °C to hydrolyze and eliminate residual Cyrene. Thus, the solvent was not recycled due to the basic elimination step.

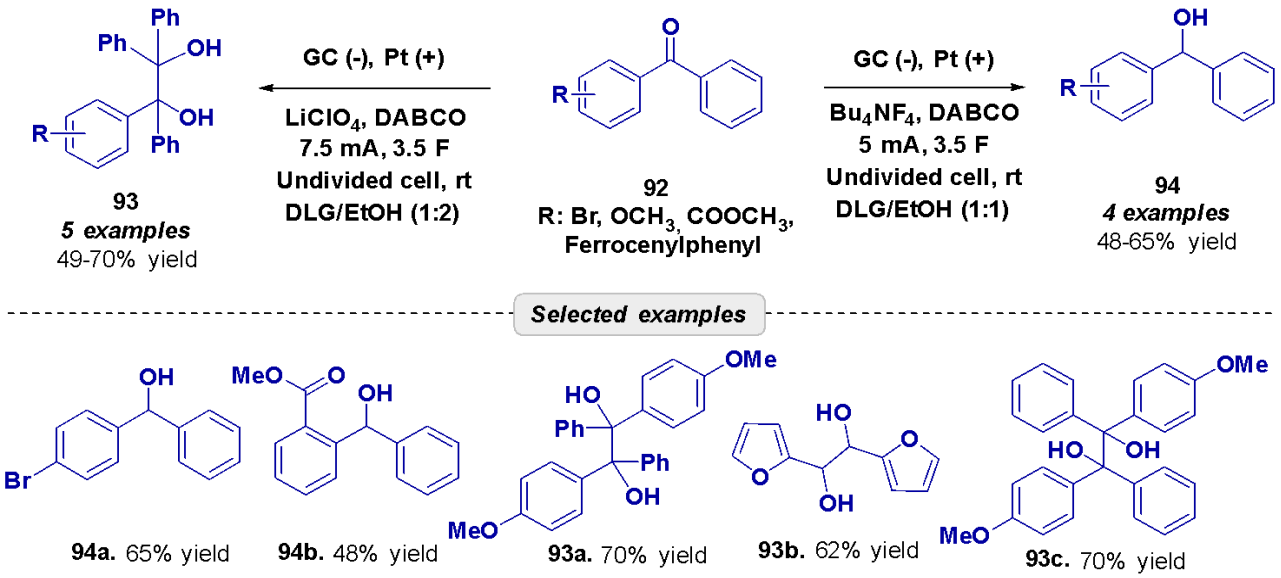

Scheme 22. Electrochemical reduction of benzophenone **92** with DLG/EtOH as solvent.

According to the authors, the presence of cyrene was essential for the selective reduction of benzophenone, because the anionic radical intermediate formed and stabilized by the Bu_4N^+ cation present in the electrical double layer when cyrene is in high concentration, facilitating the second electron transfer, producing the alcoholic derivative. With this, the reaction preferentially follows the two-electron pathway, leading to the selective formation of the diphenylmethanol derivative **94**. Furthermore, the ability of cyrene to interact with cations changes in solvent concentration or with the nature of the supporting electrolyte cation. These changes influence the balance between the single-electron or two-electron pathways. The use of supporting electrolyte lithium perchlorate ($LiClO_4$) and less concentration of cyrene occurs in the single-electron pathway, generating pinacol **93** as a main product. This occurs because the Li^+ cation has small ionic radius and high degree of solvation, causing a lower capacity to stabilize the anionic radical formed in the reduction step, leading to radical-radical coupling. This set of effects shifts the reaction making the one-electron pathway, resulting in the formation of the pinacolic **93** product. The authors did not provide any further mechanistic information and no other solvents were tested for the Li^+ system.

3.2 2-MeTHF

Colangeli and colleagues developed a protocol for electrochemical reductive amination,[76] using 4-fluorobenzaldehyde **95** and butylamine **7** to form **96** as product (Scheme 23). Various solvent mixtures were evaluated, from fossil fuels to green solvents, and 2-MeTHF afforded moderate yields, and the addition of water or methanol as cosolvents led to overreduction and loss of selectivity, probably due to biphasic conditions, increased proton availability, and less stabilization of intermediates. The use of acetonitrile and water as cosolvents restored selectivity, improving the conductivity of the medium, preventing proton donation and stabilizing the intermediate. Thus, the use of 2-MeTHF resulted in good yields and formation of byproduct **97**, with a small increase of reaction time, indicating limitations related to polarity, high ohmic resistance and ionic conductivity. With this, 2-MeTHF showed limitations with polarity and ionic conductivity, not being considered the best condition by the authors. In this case, acetonitrile and water azeotrope solution was chosen for the reaction condition, being easily recoverable and with excellent yields (**96** 76% yield, **97** byproduct 4% yield). Even with this result, 2-MeTHF still represents a viable alternative for a more sustainable organic

electrochemical synthesis. During the reaction work-up, the mixture was subjected to a simple distillation. This procedure allows the recovery of water-acetonitrile azeotrope. After diluting in ethyl acetate, filtered, and then distilled again, the product was obtained pure, and both solvents were recovered in above 80%.

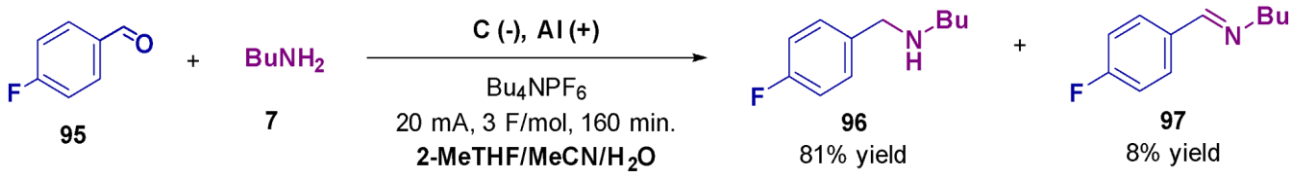

Scheme 23. Electrochemical amination of 4-fluorobenzaldehyde.

In 2022, Carvalho and coworkers demonstrated the use of 2-MeTHF as a reaction medium to promote the electrochemical cyanation of indoles, under conditions free of metal catalysts (Scheme 24).[77] The authors showed that the use of cosolvent improves the reaction conditions, as for example, 2-MeTHF/MeOH/H_2O (5/2/0.1 ratio), probably due to the fact 2-MeTHF has limitations, causing the electrolysis reaction to not occur efficiently. In this reaction, the authors used tetrabutylammonium cyanide (Bu_4NCN) with a dual function,[78] as both an electrolyte and a reagent, serving as the source for the cyanide. During the method optimization, other solvents were tested, such methanol, DCM, TFE, and a 2-MeTHF/MeOH/H_2O mixture in a 5/2/0.1 ratio showed the best result with 79% yield. The proposed mechanism started with anode oxidation of indole **98**, forming the radical cation **I**. This intermediate, an electrophilic species, is attacked by cyanide anion **II** in solution, leading to formation of a regioisomeric intermediate radical **III** or **IV**, that is subsequently oxidized at anode, generating the isomers after the loss of the proton. The reaction work-up involves dilution with DCM and washing with water. The solvents were removed under reduced pressure and purified by column chromatography. There are no reports of solvent recovery in this process.

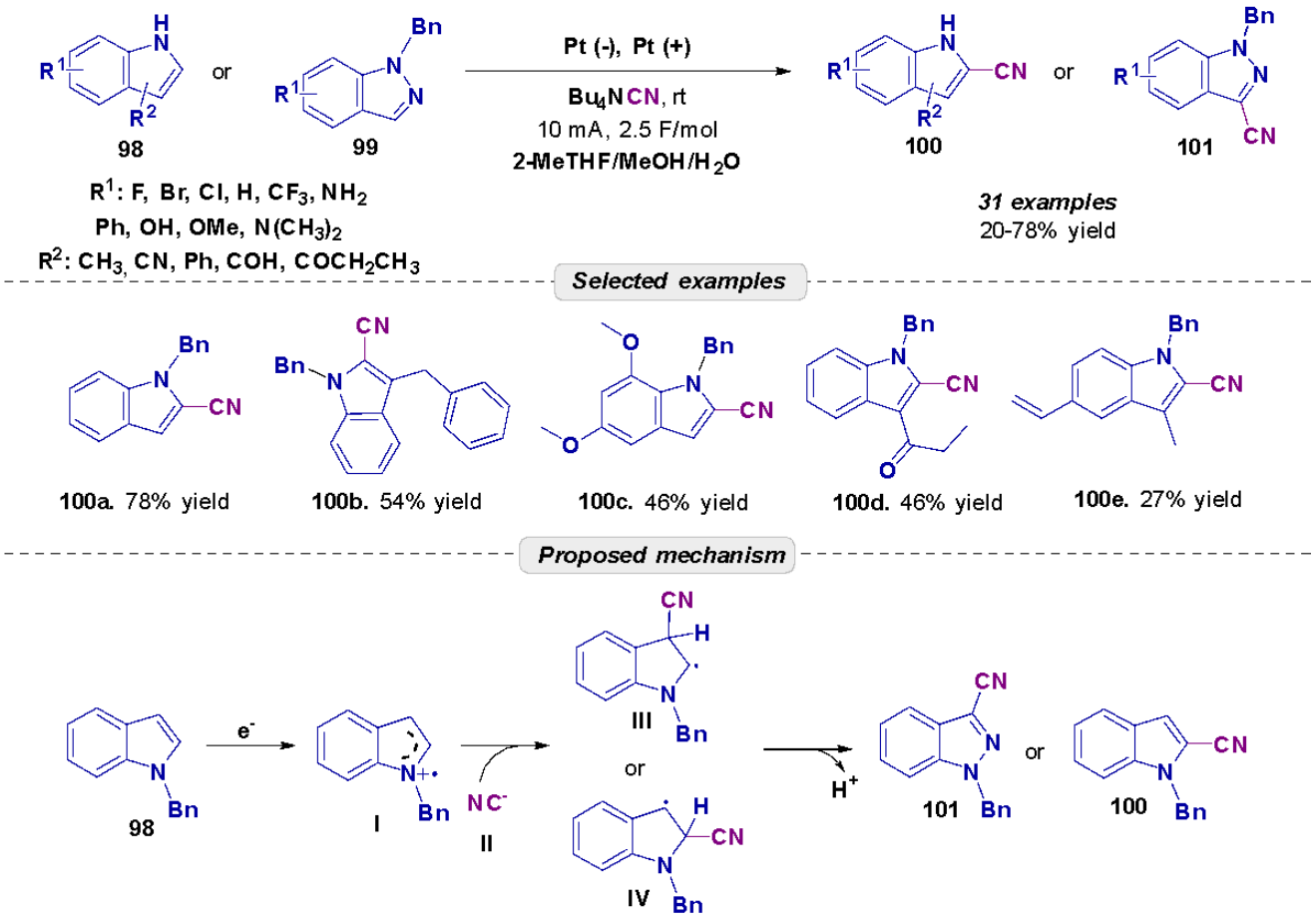

Scheme 24. Electrochemical cyanation protocol with 2-MeTHF as solvent.

3.3 Glycerol

In biodiesel production, through catalytic transesterification of triglycerides under basic conditions, glycerol is obtained as a byproduct. Thus, glycerol is generated in large quantities by the biodiesel industry, and being a waste product is discarded in large amounts. Since it is a cheap, safe, and environmentally friendly product, glycerol has been investigated as solvent in various chemical transformations.[79-82] In this context, the use of glycerol in organic reactions has been of great interest due to its chemical properties.[83] It has a high boiling point (290 °C), forming crystals at low temperatures (melting point at 17.8 °C), a density of 1.26 g.cm^{-3} at 20 °C, with an average dielectric constant of 43 at 20 °C. Furthermore, it is a non-toxic and non-flammable solvent. It can solubilize inorganic salts, acids, bases, metal complexes, and other organic compounds that are poorly miscible in water. However, due to its high viscosity (1200 cP at 20 °C), usually heating is required (>60 °C) to achieve lower viscosity or the use of cosolvents. Furthermore, the high reactivity of its hydroxyl groups can generate undesirable byproducts.[82-85] Given these physicochemical properties, glycerol has been an excellent substitute for other solvents, such as DMF and DMSO.

As far as we know, only one example of electrochemical transformation using glycerol as solvent has been reported by Ackermann and his group,[86] employing a cobalt-catalyzed C-H activation. The reaction had aromatic benzamides **102** and alkynes **103** as substrates, graphite felt (GF) as anode, platinum plate (Pt) as cathode, and cobalt (II) acetate ($Co(OAc)_2$) as catalyst, sodium pivalate (NaOPiv) as additive, in a unit cell with constant current of 4 mA at 40 °C, obtaining yields of 41 to 92% (Scheme 25). In this process, glycerol was chosen because it has a renewable origin and has good electrochemical properties. A high dielectric constant provides high ionic

conductivity, allowing electrolysis to be carried out without addition of supporting electrolytes, and glycerol does not participate competitively, being inert under electrochemical conditions. However, the use of water as a co-solvent is essential, because pure glycerol causes a drastic drop in yield due to high viscosity. In the method optimization, other solvents were applied, such as THF, DCE, TFE and 2-MeTHF aqueous solution (65% yield), as well as γ-valerolactone (GVL) and H_2O (56% yield). The authors did not provide any further mechanistic information. For the reaction work-up, after the electrolysis was complete, an extraction with DCM and water was performed, followed by purification by column chromatography. The authors did not report solvent recovery.

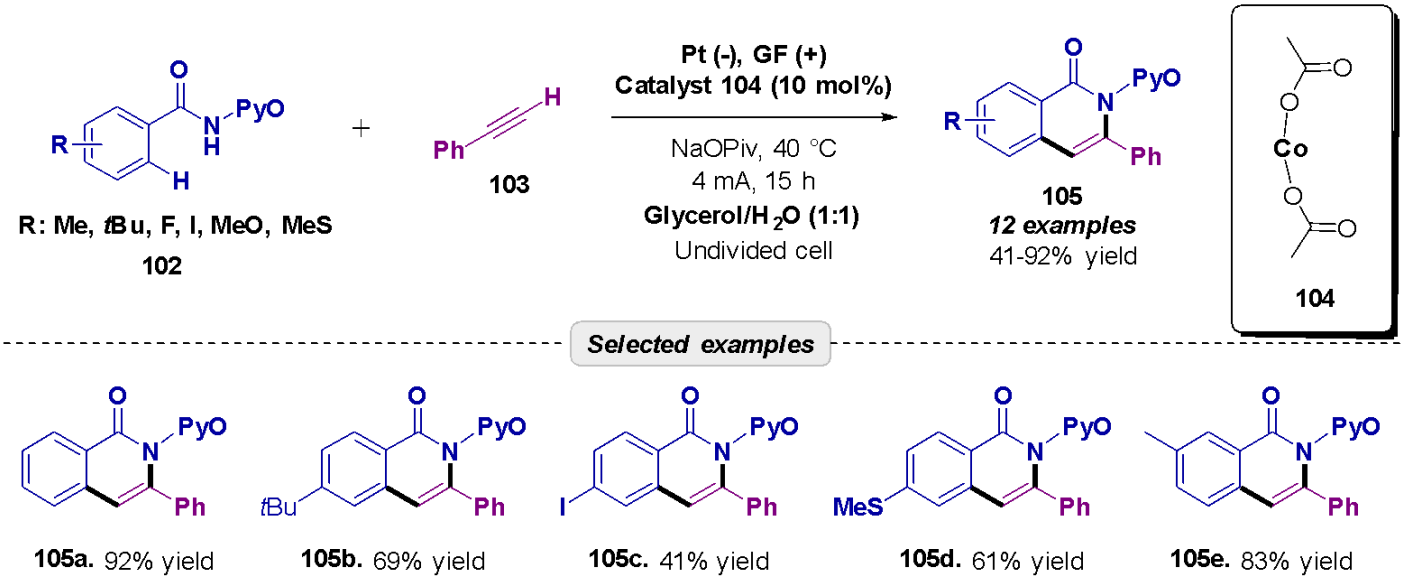

Scheme 25. Electrochemical benzamides C-H activation with alkyne in glycerol.

3.4 γ-Valerolactone

γ-Valerolactone (GVL) **110** is a versatile biomass-derived platform molecule commonly produced *via* catalytic hydrogenation of levulinic acid (LA), which itself is obtained from lignocellulosic biomass through acid-catalyzed hydrolysis and dehydration of carbohydrates (Scheme 26).[87-89] This two-step pathway (biomass to levulinic acid, followed by hydrogenation to GVL) has been widely recognized as one of the most promising valorization routes within biorefinery schemes due to its high carbon efficiency and scalability potential.[87,88]

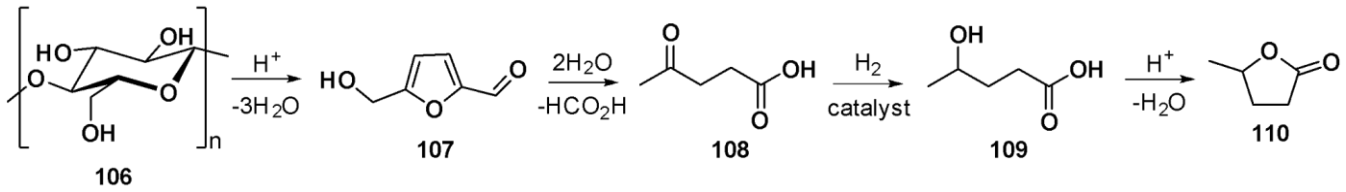

Scheme 26. General process for converting lignocellulosic biomass into GVL.

Structurally, GVL contains a five-membered lactone ring that confers moderate polarity and hydrogen-bond-accepting ability while maintaining relatively low basicity.[90] It is fully miscible with water and many organic solvents, exhibits a high boiling point (207–208 °C), a low melting point (−31 °C), and a density of approximately 1.05 g·cm^{-3} at ambient temperature.[90,91] In addition, its low vapor pressure and moderate viscosity contribute

to reduced volatility, improved handling safety, and minimized solvent losses compared with conventional volatile organic compounds (VOCs).[90,92] These physicochemical properties enable its application across a broad range of organic reactions and catalytic transformations.

GVL has been extensively investigated as a green alternative to traditional dipolar aprotic solvents such as DMF and NMP, which are associated with toxicity and regulatory concerns.[90,92] Owing to its favorable environmental profile, biodegradability, and renewable origin, GVL has demonstrated comparable or superior performance in several Nucleophilic Aromatic Substitution (S_NAr), *N*-alkylation, amidation, Pd-catalyzed coupling, hydrogenation, and biomass conversion reactions.[90,93,94]

Beyond its role as a solvent, GVL is a key C_5 platform molecule in biorefinery concepts. It readily undergoes hydrogenation, ring-opening, and deoxygenation reactions, serving as a precursor to a variety of value-added chemicals and renewable fuels.[87,88,95] Notable derivatives include 4-hydroxypentanoic acid, valerate esters (useful as fuel additives), and 2-MeTHF, a widely employed bio-based solvent obtained *via* catalytic transformation of GVL.[87,95,96]

In the context of electrosynthesis, GVL has also been explored as solvent in a limited number of transformations.[97-99] However, to the best of our knowledge, the primary electrochemical studies employing GVL as solvent were published earlier to 2020, which out the time considered in the present review. Despite this, a dedicated review about resources for sustainable C-H activation, by Ackermann's group[100], published in 2020 summarizes and discusses some electrochemical transformations performed in GVL, showing its potential in sustainable electrosynthesis and a promising alternative to conventional dipolar aprotic solvents.

4. Conclusions

This review discussed various protocols that have emerged in the literature over the past five years, focusing on photochemical and electrochemical methods using less common bio-based solvents. The landscape of these green alternatives encompasses a wide range of chemical transformations, including C-H bond activation, thioesterification, cyanation, arylation, and Minisci reactions. Furthermore, the integration of heterogeneous catalysis and enantioselective processes—specifically those employing chiral phosphoric acids—highlights the growing scope of this field. A key observation is the still timid adoption of unconventional bio-based solvents, particularly in electrochemistry. Although photochemistry shows a somewhat more consolidated presence (notably with 2-MeTHF), it is clear that the choice of solvent is often guided by method efficiency rather than a primary commitment to the principles of green chemistry. Nevertheless, the initial reports compiled here demonstrate to the scientific community that the development of efficient and environmentally friendly protocols is not only feasible, but a necessary step to move beyond the comfort zone of traditional organic solvents.

Acknowledgements

The authors acknowledge FAPESP (13/07600-3, 16/20609-8, 21/12394-0, 24/21069-3), GlaxoSmithKline, CAPES (Finance Code 001), and CNPq (303973/2023-4).

References

1. Matlin, S. A.; Mehta, G.; Krief, A. *Nature Chem.* **2016**, *8*, 393–398. https://doi.org/10.1038/nchem.2498
2. Chauhan, P.; Mahajan, S.; Enders, D. *Chem. Rev.* **2014**, *114*, 18, 8807–8864. https://doi.org/10.1021/cr500235v
3. Sheldon, R. A. *ACS Sustainable Chem. Eng*. **2018**, *6*, 1, 32–48. https://doi.org/10.1021/acssuschemeng.7b03505
4. Varma, R. S. *ACS Sustainable Chem. Eng.* **2016**, *4*, 11, 5866–5878. https://doi.org/10.1021/acssuschemeng.6b01623
5. Anastas, P.; Eghbali, N. *Chem. Soc. Rev.*, **2010**, *39*, 301-312. https://doi.org/10.1039/B918763B
6. Anastas, P. T.; Warner, J. C. *Green Chemistry: Theory and practice*, **1998**, *30*.
7. Lodh, J.; Paul, S.; Sun, H.; Song, L.; Schöfberger, W.; Roy, S. *Front. Chem.* **2023**, *10*, 956502. https://doi.org/10.3389/fchem.2022.956502
8. Zhu, C.; Ang, N. W.; Meyer, T. H.; Qiu, Y.; Ackermann, L. *ACS Cent. Sci.* **2021**, *7*, 3, 415–431. https://doi.org/10.1021/acscentsci.0c01532
9. Tay, N. E. S.; Lehnherr, D.; Rovis, T. *Chem. Rev.* **2022**, *122*, 2, 2487–2649. https://doi.org/10.1021/acs.chemrev.1c00384
10. Saraiva, M. F.; Couri, M. R. C.; Le Hyaric, M.; de Almeida, M. V. *Tetrahedron.* **2009**, *65*, 3563-3572. https://doi.org/10.1016/j.tet.2009.01.103
11. Marzo, L.; Pagire, S. K.; Reiser, O.; König, B. *Angew. Chem. Int. Ed.* **2018**, *57*, 10034-10072 https://doi.org/10.1002/anie.201709766
12. Anslyn, E. V.; Dougherty, E. V. *Modern physical organic chemistry*; University Science, 2006. Print: Sausalito, CA.
13. Jabłoński, A.; Jabłoński; A. *Nature* **1933**, *131*, 839-840. https://doi.org/10.1038/131839B0
14. Davidson, M. W. *Lab. Med.* **2009**, *40*, 694-695. https://doi.org/10.1309/lmyh007zkfvxffrc
15. Romero, N. A.; Nicewicz, D. A. *Chem. Rev.* **2016**, *116*, 10075-10166. https://doi.org/10.1021/acs.chemrev.6b00057
16. Buzzetti, L.; Crisenza, G. E. M.; Melchiorre, P. *Angew. Chem. Int. Ed.* **2019**, *58*, 3730-3747. https://doi.org/10.1002/anie.201809984
17. Lakowicz, J. R. In *Principles of Fluorescence Spectroscopy*; Springer, Boston, MA, **2006**; 277-330. https://doi.org/10.1007/978-0-387-46312-4_8
18. Arias-Rotondo, D. M.; McCusker, J. K. *Chem. Soc. Rev.* **2016**, *45*, 5803-5820. https://doi.org/10.1039/C6CS00526H
19. Lima, C. G. S.; Lima, T. D. M.; Duarte, M.; Jurberg, I. D.; Paixão, M. W. *ACS Catal.* **2016**, *6*, 1389-1407. https://doi.org/10.1021/acscatal.5b02386
20. Souza, E. R.; Sigoli, F. A. *Quím. Nova.* **2012**, *35*, 1841-1847. https://doi.org/10.1590/S0100-40422012000900024
21. Capaldo, L.; Ravelli, D. *Eur. J. Org. Chem.* **2017**, *2017*, 2056-2071. https://doi.org/10.1002/ejoc.201601485

22. Elgrishi, N.; Rountree, K. J.; McCarthy, B. D.; Rountree, E. S.; Eisenhart, T. T.; Dempsey, J. L. *J. Chem. Educ*. **2018**, *95*, 197−206. https://doi.org/10.1021/acs.jchemed.7b00361
23. Sandford, C.; Edwards, M. A., Klunder, K. J.; Hickey, D. P.; Li, M.; Barman, K.; Sigman, M. S.; White, H. S.; Minteer, S. D. *Chem. Sci.* **2019**, *10*, 6404-6422. https://doi.org/10.1039/C9SC01545K
24. Martins, G. M.; Oliveira, K. T. *Quím. Nova.* **2025**, *48*, e-20250002, 1-12. http://dx.doi.org/10.21577/0100-4042.20250002
25. Frontana-Uribe, B. A.; Little, R. D.; Ibanez, J. G.; Palma, A.; Vasquez- Medrano, R.; *Green Chem*. **2010**, *12*, 2099-2119. https://doi.org/10.1039/C0GC00382D
26. Meyer, T. H.; Choi, I.; Tian, C.; Ackermann, L.; *Chem*. **2020**, *6*, 2484-2496. https://doi.org/10.1016/j.chempr.2020.08.025
27. Capaldo, L.; Wen, Z.; Noël, T. *Chem. Sci.* **2023**,*14*, 4230-4247. https://doi.org/10.1039/D3SC00992K
28. Cembellín, S.; Batanero, B.; *Chem. Rec.* **2021**, *21*, 2453-2471. https://doi.org/10.1002/tcr.202100128
29. Horn, E. J.; Rosen, B. R.; Chen, Y.; Tang, J.; Chen, K.; Eastgate, M. D.; Baran, P. S. *Nature*. **2016,** *533*, 77-81. https://doi.org/10.1038/nature17431
30. Kawamata, Y.; Yan, M.; Liu, Z.; Bao, D.-H.; Chen, J.; Starr, J. T.; Baran, P. S. *J. Am. Chem. Soc.* **2017**, *139*, 22, 7448–7451. https://doi.org/10.1021/jacs.7b03539
31. Kärkäs, M. D. *Chem. Soc. Rev.* **2018**, *47*, 5786-5865. https://doi.org/10.1039/C7CS00619E
32. Liu, X.; Jiao, Y.; Zheng, Y.; Jaroniec, M.; Qiao, S.-Z. *Nat. Commun.* **2022**, *13*, 5471. https://doi.org/10.1038/s41467-022-33258-0
33. Liu, Y.; Xue, L.; Shi, B.; Bu, F.; Wang, D.; Lu, L.; Shi, R.; Lei, *A. Chem. Commun.* **2019**, *55*, 14922-14925. https://doi.org/10.1039/C9CC08528A
34. Maki, M. A. A.; Tan, K. F.; Yee, M. T. S.; Mishra, D. K.; Venkatesh, M. P.; Abduljaleel, O. W.; Karahan, M.; Palanirajan, V. K. *Discov. Chem.* **2025**, *2*, 342-378. https://doi.org/10.1007/s44371-025-00450-2
35. de Marco, B. A.; Rechelo, B. S.; Tótoli, E. G.; Kogawa, A. C.; Salgado, H. R. N. *Saudi Pharm. J.* **2019**, *27*, 1-8. https://doi.org/10.1016/j.jsps.2018.07.011
36. Capello, C.; Fischer, U.; Hungerbühler, K. *Green Chem.* **2007**, *9*, 927-934. https://doi.org/10.1039/b617536h
37. Pandit, B.; Saha, P. *Sust. Chem. Clim. Action.* **2025**, *7*, 100140-100157. https://doi.org/10.1016/j.scca.2025.100140
38. Quadros, G. T.; Valente, L. C. L.; Abenante, L.; Barcellos, T.; Hartwig, D.; Lenardão, E. J. *SusCirc. NOW.* **2025**, *2*, a26460474. https://doi.org/10.1055/a-2646-0474
39. Gu, Y.; Jérôme, F. *Chem. Soc. Rev.* **2013**, *42*, 9550-9570. https://doi.org/10.1039/c3cs60241a
40. Martelli, L. S. R.; Machado, I. V.; dos Santos, J. R. N.; Corrêa, A. G. *Catalysts*. **2023**, *13*, 553. https://doi.org/10.3390/catal13030553

41. Corrêa, A. G.; Paixao, M. W.; Schwab, R. S. *Curr. Org. Synth*. **2015**, *12*, 675-695. https://doi.org/10.2174/1570179412061508281021 08
42. Gomes, G. R.; Galaverna, R. S.; Pastre, J. C. In *Biomassa, Estrutura, Propriedades e Aplicações*; Gallo, J. M. R.; Corrêa, A. G., Eds.; EdUFSCar, **2020**, 45.
43. Pace, V.; Hoyos, P.; Castoldi, L.; Domínguez de María, P.; Alcántara, A. R. *ChemSusChem.* **2012**, *5*, 1369–1379. https://doi.org/10.1002/cssc.201100780
44. Aycock, D. F. *Org. Process Res. Dev.* **2007**, *11*, 156–159. https://doi.org/10.1021/op060155c
45. Santoro, S.; Ferlin, F.; Luciani, L.; Ackermann, L.; Vaccaro, L. *Green Chem.* **2017**, *19*, 1601–1612. https://doi.org/10.1039/C7GC00067G
46. Calvo-Flores, F. G.; Monteagudo-Arrebola, M. J.; Dobado, J. A.; Isac-García, J. *Top. Curr. Chem.* **2018**, *376*, 18. https://doi.org/10.1007/s41061-018-0191-6
47. Xu, X.-M.; Wang, J.; Chen, S.; Chen, X.; Chen, J.; Liu, Q.; Wang, Z.; Tian, M.; Sun K. *Adv. Synth. Catal.* **2025**, *367*, e202401516. https://doi.org/10.1002/adsc.202401516
48. Kamal, A.; Singh, H. K.; Maury, S. K.; Kushwaha, A. K.; Srivastava, V.; Singh, S. *Asian J. Org. Chem.* **2023**, *12*, e202200632. https://doi.org/10.1002/ajoc.202200632
49. Meng, X.-X.; Kang, Q.-Q.; Zhang, J.-Y.; Li, Q.; Wei, W.-T.; He, W-M. *Green Chem.* **2020**, *22*, 1388–1392. https://doi.org/10.1039/C9GC03769A
50. Yue, T.; Zhang, S.-Z.; Li, M.-M.; Zhang, Z.-H. *ChemSusChem.* **2025**, *18*, e202501607. https://doi.org/10.1002/cssc.202501607
51. Gui, Q.-W.; Teng, F.; Li, Z.-C.; Xiong, Z.-Y.; Jim, X.-F.; Lin, Y.-W.; Cao, Z.; He, W.-M. *Chin. Chem. Lett.* **2021**, *32*, 1907–1910. https://doi.org/10.1016/j.cclet.2021.01.021
52. Shi, T.; Tian, M.; Zhu, Y.; Sun, L.; Liu, F.; Chen, S.; Hao, E.; Sun, K.; Wang, X. *J. Org. Chem.* **2025**, *90*, 3435–3443. https://doi.org/10.1021/acs.joc.4c03187
53. Li, L.; Li, J.-Z.; Sun, Y.-B.; Luo, C.-M.; Qiu, H.; Tang. K.; Liu, H.; Wei, W.-T. *Org. Lett.* **2022**, *24*, 4627–4631. https://doi.org/10.1021/acs.orglett.2c01977
54. Lu, C.; Chen, R.; Wang, R.; Jing, D.; Zheng, K. *Org. Lett.* **2023**, *25*, 871–875. https://doi.org/10.1021/acs.orglett.2c04189
55. He, Z.-W.; Yuan, B.-R.; Yu, X.-Y.; Jiang, M.; Chen, J.-R.; Xiao, W.-J. *Angew. Chem. Int. Ed.* **2025**, *64*, e202514155. https://doi.org/10.1002/anie.202514155
56. Gui, Q.-W.; Teng, F.; Yu, P.; Wu, Y.-F.; Nong, Z.-B.; Yang, L.-X.; Chen, X.; Yang, T.-B.; He, W.-M. *Chin. J. Catal.* **2023**, *47*, 246–255. https://doi.org/10.1016/S1872-2067(22)64162-7
57. Zheng, W.; Xu, Y.; Lin, L. *ChemPhotoChem.* **2022**, *6*, e202100264. https://doi.org/10.1002/cptc.202100264
58. Sagadevan, A.; Charitou, A.; Wang, F.; Ivanova, M.; Vuagnat, M.; Greaney, M. F. *Chem. Sci.* **2020**, *11*, 4439–4443.

https://doi.org/10.1039/D0SC01289K
59. Peng, Q.-H.; Jiang, J.; Liao, Z.-H.; Wu, Z.-L.; Ou, L.-J.; Dai, H.; Peng, J.; He, W.-M. *ACS Sustainable Chem. Eng.* **2025**, *13*, 10971-10977. https://doi.org/10.1021/acssuschemeng.5c03350
60. Sun, Y.; Song, G.; Yan, Y.; Kang, T.; Dong, J.; Li, G.; Xue, D. *Green Chem.* **2025**, *27*, 5315–5321. https://doi.org/10.1039/D5GC00566C
61. Skolia, E.; Gkizis, P. L.; Kokotos, C. G. *Org. Biomol. Chem.* **2022**, *20*, 5836. https://doi.org/10.1039/d2ob01066f
62. Zhang, Y.; Li, Y.; Ni, S.-F.; Li, J.-P.; Xia, D.; Han, X.; Lin, J.; Wang, J.; Das, S.; Zhang, W.-D. *Chem. Sci.* **2023**, *14*, 10411. https://doi.org/10.1039/d3sc04188c
63. Meng, X.-C.; Pan, T.-X.; Yang, F.; Zhu, H.-X.; Huang, Y.-W.; Leng, B.-R.; Wang, D.-C.; Zhu, Y.-L. *J. Org. Chem.* **2025**, *90*, 1061–1070. https://doi.org/10.1021/acs.joc.4c02462
64. Dai, J.-L.; Wang, T.; Hao, Y.; Zhang, Y.; Yan, S.; Li, G.; Wang, J.-Y. *J. Org. Chem.* **2024**, *89*, 15901–15913. https://doi.org/10.1021/acs.joc.4c02065
65. Pereira, C. S. M.; Silva, V. M. T. M.; Rodrigues, A. E. *Green Chem.* **2011**, *13*, 2658-2671. https://doi.org/10.1039/C1GC15523G
66. Clark, J. H.; Tavener, S. J. *Org. Process Res. Dev.* **2007**, *11*, 1, 149–155. https://doi.org/10.1021/op060160g
67. Dolzhenko, A. V. *Sustain. Chem. Pharm.* **2020**, *18*, 100322. https://doi.org/10.1016/j.scp.2020.100322
68. Zhang, Z.-H..; Mo, J.-M..; Di, J.-Q..; Chen, M.-N. *Tetrahedron*. **2020**, *76*, 131059. https://doi.org/10.1016/j.tet.2020.131059
69. Mohamadpour, F. *Dyes Pigm.* **2021**, *194*, 109628. https://doi.org/10.1016/j.dyepig.2021.109628
70. Mohamadpour, F. *J. Photochem. Photobiol*. **2021**, *407*, 113041. https://doi.org/10.1016/j.jphotochem.2020.113041
71. Kong, D.; Dolzhenko, A. V. *Sustain. Chem. Pharm.* **2022**, *25*, 100591. https://doi.org/10.1016/j.scp.2021.100591
72. Sherwood, J.; De bruyn, M.; Constantinou, A.; Moity, L.; McElroy, C. R.; Farmer, T. J.; Duncan, T.; Raverty, W.; Hunt, A. J.; Clark, J. H. *Chem. Commun.* **2014**, *50*, 9650-9652. https://doi.org/10.1039/C4CC04133J
73. Ramos-Villaseñor, J. M.; Sotelo-Gil, J.; Rodil, S. E.; Frontana-Uribe, B. A. *Faraday Discuss*., **2023**, *247* https://doi.org/10.1039/D3FD00064H
74. Cseri, L.; Szekely, G. *Green Chem.* **2019**, *21*, 4178-4188. https://doi.org/10.1039/C9GC01958H
75. Panjalingam, S. P.; Penert, P.; Esser, B.; Winter, M.; Bieker, P. *ACS Appl. Energy Mater.* **2025**, *8*, 17, 12534–12542. https://doi.org/10.1021/acsaem.5c01216
76. Colangeli, S. T.; Campana, F.; Ferlin, F.; Vaccaro, L. *Green Chem.* **2025**, *27*, 633-641. https://doi.org/10.1039/D4GC04847D
77. Carvalho, M.-A.; Demin, S.; Martinez-Lamenca, C.; Romanov-Michailidis, F.; Lam, K.; Rombouts, F.; Lecomte, M. *Chem. Eur. J.* **2022**, *28*, e202103384.

https://doi.org/10.1002/chem.202103384
78. Gombos, L. G.; Nikl, J.; Waldvogel, S. R. *Chem. Electro. Chem.* **2024**, *11*, e202300730. https://doi.org/10.1002/celc.202300730
79. Cintas, P.; Tagliapietra, S.; Gaudino, E. C.; Palmisano, G.; Cravotto, G. *Green Chem.* **2014**, *16*, 1056-1065. https://doi.org/10.1039/C3GC41955J
80. Nebra, N; García-Álvarez, J. *Molecules*. **2020**, *25*, 2015-2033. https://doi.org/10.3390/molecules25092015
81. Narasimhamurthy, K. H.; Joy, M. N.; Sajith, A. M.; Santra, S.; Zyryanov, G. V.; Swaroop, T. R.; Rangappa, K. S. *Lett. Org. Chem.* **2023**, *20*, 945-957. https://doi.org/10.2174/1570178620666230418093820
82. Ravichandiran, P.; Gu, Y. *Bio-Based Solvents*, **2017**, 1. https://doi.org/10.1002/9781119065357.ch1
83. Díaz-Álvarez, A. E.; Francos, J.; Lastra-Barreira, B.; Crochet, P.; Cadierno, V. *Chem. Commun.* **2011**, *47*, 6208–6227. https://doi.org/10.1039/C1CC10620A
84. Gu, Y.; Jerome, F. *Green Chem.* **2010**, *12*, 1127–1138. https://doi.org/10.1039/C001628D
85. Oliveira, A. N.; Melchiorre, M.; Costa, A. A. F.; Silva, L. S.; Paiva, R. J.; Auvigne, A.; Ouyang, W.; Luque, R.; Filho, G. N. R.; Noronha, R. C. R.; Espósito, R.; Nascimento, L. A. S.; Len, C. *Sustain. Chem. Pharm.* **2024**, *41*, 101656. https://doi.org/10.1016/j.scp.2024.101656
86. Meyer, T. H.; Chesnokov, G. A.; Ackermann, L. *ChemSusChem.* **2020**, *13*, 668 – 671. https://doi.org/10.1002/cssc.202000057
87. Alonso, D. M.; Bond, J. Q.; Dumesic, J. A. *Green Chem.* **2010**, *12*, 1493-1513. https://doi.org/10.1039/c004654j
88. Lange, J. P.; Van Der Heide, E.; Van Buijtenen, J.; Price, R. *ChemSusChem.* **2012**, *5*, 150-166. https://doi.org/10.1002/cssc.201100648
89. Bozell, J. J.; Petersen, G. R. *Green Chem.* **2010**, *12*, 539-554. https://doi.org/10.1039/b922014c
90. Jessop, P. G. *Green Chem.* **2011**, *13*, 1391-1398. https://doi.org/10.1039/c0gc00797h
91. Horváth, I. T.; Mehdi, H.; Fábos, V.; Boda, L.; Mika, L. T. *Green Chem.* **2008**, *10*, 238-242. https://doi.org/10.1039/b712863k
92. Henderson, R. K.; Jiménez-González, C.; Constable, D. J. C.; Alston, S. R.; Inglis, G. G. A.; Fisher, G.; Sherwood, J.; Binks, S. P.; Curzons, A. D. *Green Chem.* **2011**, *13*, 854-862. https://doi.org/10.1039/c0gc00918k
93. Tang, X.; Zeng, X.; Li, Z.; Hu, L.; Sun, Y.; Liu, S.; Lei, T.; Lin, L. *Renew. Sustain. Energy Rev.* **2014**, *40*, 608-620. https://doi.org/10.1016/j.rser.2014.07.209
94. Sinha, S.; Obkircher, M.; Deokar, R.; Yaragani, M.; R, T.; Cooper, J. γ-Valerolactone (GVL): Bio-Based Dipolar Aprotic Solvent for More Sustainable Synthesis.
95. Bond, J. Q.; Alonso, D. M.; Wang, D.; West, R. M.; Dumesic, J. A. *Science.* **2010**, *327*, 1110-1114. https://doi.org/10.1126/science.1184362
96. Pace, V.; Hoyos, P.; Castoldi, L.; Domínguez De María, P.; Alcántara, A. R. *ChemSusChem.* **2012**, *5*, 1369-1379.

https://doi.org/10.1002/cssc.201100780
97. Boissou, F.; Baranton, S.; Tarighi, M.; Vigier, K. O.; Countanceau, C. *J. Electroanal. Chem.* **2019**, *848*, 113257. https://doi.org/10.1016/j.jelechem.2019.113257
98. Sauermann, N.; Mei, R.; Ackermann, L. *Angew. Chem. Int. Ed.* **2018**, *57*, 5090–5094. https://doi.org/10.1002/ange.201802206
99. Tian, C.; Dhawa, U.; Struwe, J.; Ackermann, L. *Chin. J. Chem.* **2019**, *37*, 552-556. http://dx.doi.org/10.1002/cjoc.201900050
100. Samanta, R. C.; Meyer, T. H.; Siewert, I.; Ackermann, L. *Chem. Sci.* **2020**, *11*, 8657-8670. https://doi.org/10.1039/D0SC03578E

Authors' Biographies

Jhonathan Santos completed his bachelor's degree in Chemistry at the Pontifical Catholic University of Goiás (Brazil) in 2018 and his master's degree in Chemistry at the State University of Goiás (Brazil) in 2020. During his master's degree, he specialized in the synthesis of heterocycles through multicomponent reactions. In 2025, he completed his PhD in Science at the Federal University of São Carlos (Brazil), under the supervision of Prof. Arlene G. Corrêa. Currently, his academic work focuses on the link between more sustainable organic synthesis and medicinal chemistry.

Carlos Eduardo Tomé Rosa obtained his bachelor's degree in Industrial Chemistry from the Federal University of Catalão (Brazil) in 2025. He is currently pursuing a direct Ph.D. in Science at the Federal University of São Carlos (Brazil), under the supervision of Prof. Arlene G. Corrêa. His research focuses on the electrochemical synthesis of carboxylic acids using carbon dioxide in complex *N*-heteroaromatic compounds.

Éverton Alves Tordato obtained his Bachelor's degree in Chemistry with technological specialization from the Hermínio Ometto University Center – FHO Uniararas in 2015. He subsequently earned his Master's degree in Chemistry from the Institute of Chemistry at São Paulo State University - UNESP in 2018, followed by a Ph.D. in Science from the Department of Chemistry at Federal University of São Carlos - UFSCar in 2024. He is currently undertaking postdoctoral research at the University of São Paulo - USP and serves as a research collaborator at UFSCar. His research activities are primarily focused on studies with gliflozins, as well as on the synthesis and photochemical functionalization of β- and γ-lactams.

Arlene Gonçalves Corrêa received her B.Sc. (1985) and M.Sc. (1988) degrees from the Federal University of São Carlos - UFSCar (Brazil), conducting undergraduate research with Professor Ursula Brocksom. After spending two years as a postgraduate student in the group of Professor Andrew E. Greene at the University of Grenoble (France), she received her Ph.D. degree in 1991 under the supervision of Professor Timothy J. Brocksom at UFSCar, where she became an Assistant Professor in 1992 and Full Professor in 2014. She joined the group of Professor Paul A. Wender at Stanford University (USA) as a visiting scholar in 1996. She is the Director of the Centre of Excellence for Research in Sustainable Chemistry (CERSusChem).